2008

Experimental investigation of the Qu Tube heat pipe

Sean F. Entrekin

EXPERIMENTAL INVESTIGATION OF THE QU TUBE HEAT PIPE

by

SEAN F. ENTREKIN

A THESIS

Submitted in partial fulfillment of the requirements
for the degree of Master of Science in Engineering
in
The Department of Mechanical and Aerospace Engineering
to
The School of Graduate Studies
of
The University of Alabama in Huntsville

HUNTSVILLE, ALABAMA

2008

In presenting this thesis in partial fulfillment of the requirements for a master's degree from the University of Alabama in Huntsville, I agree that the Library of this University shall make it freely available for inspection. I further agree that permission for extensive copying for scholarly purposes may be granted by my advisor or, in his/her absence, by the Chair of the Department of the Dean of the School of Graduate Studies. It is also understood that due recognition shall be given to me and to The University of Alabama in Huntsville in any scholarly use which may be made of any material in this thesis.

Sean Entsminger

(student signature)

9/17/08

(date)

THESIS APPROVAL FORM

Submitted by Sean Entrekin in partial fulfillment of the requirements for the degree of Master of Science in Engineering and accepted on behalf of the Faculty of the School of Graduate Studies by the thesis committee.

We, the undersigned members of the Graduate Faculty of The University of Alabama in Huntsville, certify that we have advised and/or supervised the candidate on the work described in this thesis. We further certify that we have reviewed the thesis manuscript and approve it in partial fulfillment of the requirements for the degree of Master of Science in Engineering.

James B. Blackmon 10/10/08 Committee Chair
(Date)

Francis C. Wessling

Robert A Frederick Jr

Kirk Frank 10/16/08 Department Chair

College Dean

Allen M. Moriarity 12/4/08 Graduate Dean

ABSTRACT

The School of Graduate Studies
The University of Alabama in Huntsville

Degree Master of Science in Engineering College/Dept. Engineering/Mechanical and Aerospace Engineering

Name of Candidate Sean Fitzpatrick Entrekin

Title Experimental Investigation of the Qu Tube Heat Pipe

A versatile experimental apparatus was designed and fabricated in order to systematically evaluate a claimed solid-state Qu Tube heat pipe. The rotatable apparatus included a heat rate capability of 5,000W, a calorimeter, and thermistors calibrated to ± 0.1ºC. Instrumentation accuracy was evaluated using a copper rod and a copper tube of the same dimensions as the Qu Tubes being studied. Results showed that the apparatus allows excellent repeatability of data and provides the capability to determine temperature differences on the tube to ± 0.14ºC. Qu Tube results showed a gravity-dependence that caused the Qu Tube to perform like an ordinary copper tube when horizontal and when the heated end was above the cooled end. However, the Qu Tube results also showed an essentially constant temperature along the length of the tube when the Qu Tube was at a 45º angle and the heated end was below the cooled end. This essentially constant temperature demonstrates a very high thermal conductivity value; the maximum axial heat flux achieved for these tests was 650 W/cm^2.

Abstract Approval: Committee Chair James B. Blackmon

Department Chair Kirk Frankie

Graduate Dean Sheila M. Moisuddin

ACKNOWLEDGMENTS

Firstly, I want to thank my parents for always being there to encourage me and give me advice. I would like to thank Dr. Clark Hawk for hiring me to work for the Propulsion Research Center (PRC) as an undergraduate student in 2003, and deciding to keep me on as a graduate student. At my first PRC staff meeting, Dr. Hawk announced I was available for free labor to whomever needed it. Afterwards, Dr. Jim Blackmon introduced himself, and asked me if I wanted to work for him. Since that moment, and I am sure for many more years to come, I have learned so much from Drs. Hawk and Blackmon. Without Dr. Blackmon's guidance, I would not be the primary inventor on at least one patent, or know as much as I do about the business side of engineering.

I am grateful to the other professors on my committee, Drs. Coleman, Wessling, and Frederick, for their time, guidance, and for keeping me focused and on track with my research. They have also provided great encouragement.

Steve Collins in the UAH Engineering Design and Prototyping Facility helped me out so many times that I lost count. I thank you for all of your help and seemingly unending patience with me.

My research could not have been conducted without Dr. Connie Carrington at NASA. She gave Dr. Blackmon the first amount of seed money to start studying the Qu Tube, which allowed me to be hired, and has given us great support and direction.

And lastly, Dr. David Lineberry for listening to problems I was having with research hardware, data analysis, writing my thesis, etc.

TABLE OF CONTENTS

List of Figures viii

List of Tables xi

List of Symbols xii

Chapter

1 Introduction 1

1.1 Liquid – Vapor Heat Pipes 3

1.2 Pumped Loop Heat Pipes 5

2 Design of Experimental Test Apparatus 7

2.1 Experiment Rationale 10

2.2 Approach 11

2.3 Cylindrical Conduction Analysis 27

3 Calibration and Uncertainty Analysis 29

3.1 Generation of Individual Thermistor Coefficients 32

3.2 Calibration Coefficients Checkout Tests 33

3.3 Uncertainty Analysis 34

4 Test Protocol 37

5 Results and Discussion 39

5.1 Copper Rod 42

5.2 Copper Tube 47

5.3 Qu Tube 47

6 Conclusions and Recommendations 54

Appendix A: Qu Energy Website 58

Appendix B: Cylindrical Radial Conduction Analysis 61

Appendix C: Procedure for Installation of Test Article 64

Appendix D: Analysis for Insulated Solid and Annular Fin Temperature Gradient 67

REFERENCES 72

LIST OF FIGURES

Figure		Page
1.1	Schematic of Conventional Liquid Vapor Heat Pipe	5
1.2	Schematic of Loop Heat Pipe	6
2.1	T(x) for a Copper Tube Fin Compared with Experimental Data	9
2.2	Rotatable Heat Pipe Experimental Apparatus	11
2.3	Digital Protractor Used to Measure the Angle of the Test Article	11
2.4	2kW Coil Heaters	13
2.5	Copper Bar with Two Thermocouple Holes	13
2.6	3-Phase Power Controller and Diagram of Coil Heaters Wired in a Delta Configuration	13
2.7	Wattnode Power Meter Inside Enclosure	13
2.8	Enclosure Containing Power Controller Next to PID Controller	14
2.9	Three AC Variable Transformers with Power Meters	15
2.10	DC Power Supply Used for Low Power Tests	15
2.11	Mineral Wool Insulation	16
2.12	Custom Insulation Jacket Wrapped Around Mineral Wool and Coil Heater	16
2.13	Cross Section of Heater Coil and Insulation	16
2.14	CPVC Calorimeter	18
2.15	Water Filter, Pressure Regulator, Flowmeter, and Thermistor Assembly	18
2.16	Copper Fin Sections	19
2.17	Foam Insulated Calorimeter	19
2.18	Cross Section of Thermistor Rake and Insulation	21

2.19 Side View of Thermistor Rake CAD Drawing Showing Spring and Teflon Pin . 21
2.20 Delrin Thermistor Rake Showing White Teflon Pins and Thermistor Grooves... 21
2.21 Top Half of Delrin Thermistor Rake 22
2.22 Assembled Delrin Thermistor Rake with Thermistors 22
2.23 Custom ULTRA Jacket Insulation for Delrin Thermistor Rakes (shown unwrapped) 22
2.24 National Instruments SCXI-1000 with Digitizer 24
2.25 LabVIEW 8 Block Diagram Code 25
2.26 LabVIEW Front Panel 26
2.27 Drawing of Omega Series 44032 Thermistor 27
3.1 Copper Calibration Part in CNC Mill 30
3.2 Slots for Thermistor Wires Being Machined into Calibration Part 30
3.3 Thermistors in Copper Calibration Part with Thermal Grease 31
3.4 Foamboard Box Containing Copper Calibration Part with Thermistors 32
3.5 Resistance vs. Time Collected During Calibration in Environmental Chamber .. 32
3.6 Comparison of Different Thermistor Coefficient Methods 34
5.1 Cross Section of Insulated Annular Fin Used in Analysis..... 41
5.2 Results of Insulated and Uninsulated Solid Rod Fin Analysis with Experimental Data 41
5.3 Results of Insulated and Uninsulated Annular Fin Analysis with Experimental Data 42
5.4 Data for Horizontal Copper Rod..... 44
5.5 Data for Copper Rod at +45 degree Inclination..... 45

5.6 Data for Copper Rod at -45 degree Inclination 45

5.7 Thermistor Temperature vs. Angle for Copper Rod 46

5.8 Thermistor Temperature vs. Angle for Copper Rod with Added Insulation 46

5.9 Results for Copper Tube 47

5.10 Averaged T(x) for Qu Tube at Three Test Positions with Constant Power 49

5.11 Difference in Horizontal Qu Tube Temperature Divided by Distance Between Thermistors 50

5.12 Difference in -45° Qu Tube Temperature Divided by Distance Between Thermistors 50

5.13 Difference in +45° Qu Tube Temperature Divided by Distance Between Thermistors 51

5.14 Difference in Temperature for Qu Tube and Copper Tube 51

5.15 Difference in Temperature Divided by Distance Between Thermistors for Qu Tube and Copper Tube 52

5.16 Temperature vs. Time for the twenty-seven thermistors during a high heat rate test of the Qu Tube 52

5.17 Temperatures for Water In and Out, and Selected Thermistors, Along with Power Out Over a Steady-State Period of Time 53

D.1 Analysis for insulated solids and annular fin temperature gradient 68

LIST OF TABLES

Table **Page**

2.1 Resistance Versus Temperature for Omega Series 44032 Thermistor 27

3.1 Average and Standard Deviation for Each Method Used to Determine Thermistor Calibration..... 34

LIST OF SYMBOLS

A	Area
A_c	Cross-Sectional Area
$(B_i)_k$	Elemental Systematic Uncertainties
B_J	Systematic Uncertainty
B_T	Systematic Uncertainty in Temperature Measurement
$B_{\Delta T}$	Systematic Uncertainty in Temperature Difference
c_p	Specific Heat Capacity
h	Heat Transfer Coefficient
k	Thermal Conductivity
L	Length
$\dot{m}$	Mass Flow Rate
P	Perimeter
q	Heat Rate
r	Radius
R	Resistance
T	Temperature
T_b	Base Temperature
T_{In}	Temperature of Water Flowing Into Calorimeter
T_∞	Ambient Temperature
T_{Out}	Temperature of Water Flowing Out of Calorimeter
θ	Excess Temperature

θ_b Excess Temperature at Base

θ_T Derivative of ΔT with Respect to T

U Heat Transfer Coefficient

U_{eq} Equivalent Heat Transfer Coefficient

CHAPTER 1

INTRODUCTION

A new type of heat pipe, known as a Qu Tube, was claimed to operate by a solid-state heat transfer mechanism that produced an exceptionally high effective thermal conductivity and axial heat flux. These extraordinary claims, substantiated in part by some early observations made by the University of Alabama in Huntsville (UAH), were the impetus for further study of the Qu Tube. Exploratory testing of the Qu Tube solid state heat pipe began in the spring of 2003 as part of a NASA grant through the National Space Science and Technology Center (NSSTC), grant number NCC8-200. UAH was provided with three Qu Tubes 18" in length and 5/16" in diameter. No information was given about these initial tubes, only that they contained a solid-state heat transfer material instead of a working fluid like a conventional heat pipe. Patents granted to the tube's inventor[1,2,3,4], were consulted to ascertain the mechanism of heat transfer. However, reading the patents most often just led to more questions about the technology. Initial checkout tests were conducted on these tubes by inserting part of the tube into boiling water, and measuring the temperature of the exposed end with K-type thermocouples. These initial tests indicated extremely rapid temperature increases with essentially constant temperature along the part of the tube exposed to the ambient air, but this did not prove that the Qu Tube was anything more than a conventional heat pipe. Testing

progressed to more controlled experiments utilizing electric band heaters and a vacuum chamber. Results again showed an essentially constant temperature along the tube with temperature differences that were well within the uncertainty of the thermocouples. In some cases, the temperature at the end of the tube opposite of the heater was greater than the temperature closest to the heater, but not by more than the thermocouple uncertainty. The nearly constant temperature along the length of the tube made the determination of thermal conductivity by traditional methods, such as using heat flux and measured temperature differences, impractical, especially using thermocouples. The short length of the tubes was also a hindrance in that it offered little surface area for heat transfer, and limited area for instrumentation, and thus a calorimeter could not be used to determine the heat rate. In order to estimate the thermal conductivity of these relatively short Qu Tubes, other analysis tools were tried, such as the Forbes Method and the Ingenhous Technique, but the only method that was practical was based on using multiples of the thermal conductivity of copper to obtain the essentially constant temperature along the heated tube.

Some performance characteristics of the Qu Tube were passed along to UAH anecdotally. One such property was the ability of the heat transfer mechanism to function up to the melting point of the container material. This claim was somewhat demonstrated at UAH after the tip of a Qu Tube was inadvertently melted by a torch during a high heat flux test. Up to the point where the tube burst, the temperatures were essentially the same for the portion of the tube a few inches from the area of the tube that was being heated to the far tip. However, this did not prove that the heat transfer mechanism was anything other than that of a conventional heat pipe. A conventional

heat pipe undergoing excessive heat transfer and "burn out" with liquid not reaching the evaporator section could behave in the same way. There were also data from other studies, including earlier work done at SRI, which showed a sinusoidal temperature distribution along the Qu Tube.* UAH has observed instances in which the tube was at a steady-state temperature and then would suddenly jump without a change in power input, flowrate, surrounding temperature, or angle. These observations and anecdotes emphasized the need for a very well-calibrated set of temperature measurements using thermistors instead of thermocouples. More accurate instrumentation, with longer tubes and higher heat rates, would presumably enable the measurement of the very small temperature gradients that were expected.

1.1 Liquid – Vapor Heat Pipes

A liquid – vapor, or pool boiler, heat pipe is able to achieve higher axial heat fluxes than thermal conduction, and is able to maintain a nearly constant temperature along the entire length of the tube. It does this by heating a working fluid inside of the pipe, which causes the liquid to evaporate. The vapor travels along the essentially adiabatic length of the pipe to the opposite end where heat is removed, causing the vapor to condense. How fast the vapor travels is governed by the difference in vapor pressure between the evaporator and the condenser, the dimensions of the pipe, and the operational temperature.[5] The condensate wicks back down by capillary action or gravity. This process is shown in Figure 1.1. There are four common types of wick

---

* We have seen these data in a Stanford Research Institute report of the Qu Tube, but we are not at liberty to provide this information due to a non-disclosure agreement. Parts of the report are cited on a website included in Appendix A.

structures: groove, wire mesh, powdered metal, and fiber string.[5] Each type has its own advantages and disadvantages, and its own capillary limit (the rate at which the working fluid travels from the condenser to the evaporator through the wick) which is a reciprocal function of the heat pipe's length, and thus longer heat pipes transport less heat than shorter heat pipes.[5]

A vacuum is pulled inside of the tube to control the temperature at which the liquid vaporizes. This is often referred to as tuning a heat pipe, and is one of the drawbacks, given that heat pipes are often custom-made for a specific application. If a heat pipe is subjected to a temperature that is outside of its tuned range, the working fluid can vaporize completely and the pipe becomes overheated, and the heat transfer between the condenser and evaporator is disrupted.[5]

Conventional heat pipes are adversely affected by operation with the evaporator above the condenser in a gravity environment because they cannot generate sufficient capillary pumping pressure to overcome the gravity head in this orientation. Smaller pore size can increase the capillary pumping force, but this limits the length of the heat pipe because the liquid flow pressure losses through the wick associated with the smaller pore size rapidly become a factor affecting heat transport capability[6].

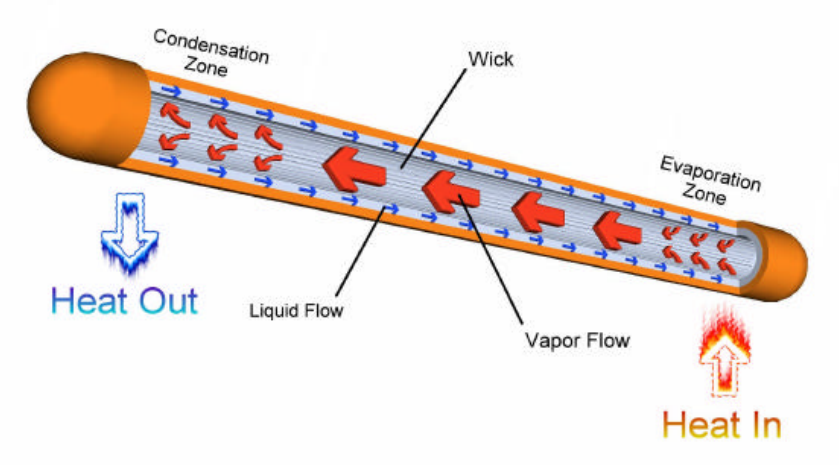

Figure 1.1 - Schematic of Conventional Liquid Vapor Heat Pipe[2]

1.2 Pumped Loop Heat Pipes

Pumped loop heat pipes are better than liquid-vapor heat pipes at transferring heat longer distances. There are two basic types of loop heat pipes, capillary pumped loops (CPLs) and loop heat pipes (LHPs). The main difference between the two types is that in a CPL the reservoir is a separate chamber where the liquid accumulates and is actively controlled, unlike in a LHP with the reservoir integrally connected to the evaporator. Figure 1.2 shows a schematic of a LHP. Once the liquid is evaporated in a LHP, the vapor flows into the outer annulus through the grooves in a porous insert. As the vapor travels the length of the evaporator, it becomes slightly superheated because the inner wall temperature of the evaporator is higher than the saturation temperature. The pressure difference between the condenser and the evaporator forces the vapor into the vapor line. When the vapor reaches the condenser, the working fluid condenses onto tapered walls and flows down by gravity and capillary pressure and is subcooled. The subcooled liquid returns to the reservoir by the capillary pumping pressure of the wick structure. Working fluid is distributed to the evaporator from the reservoir through a

small annulus. If the reservoir were drained completely, there would still be enough liquid to saturate the wick, making the LHP self-priming.[7] Loop heat pipes, particularly CPLs, are more complicated to build and operate than conventional heat pipes.[7] However, there are no liquid entrainment losses from a liquid-vapor interface, or losses due to a wicking structure found in conventional heat pipes.[7]

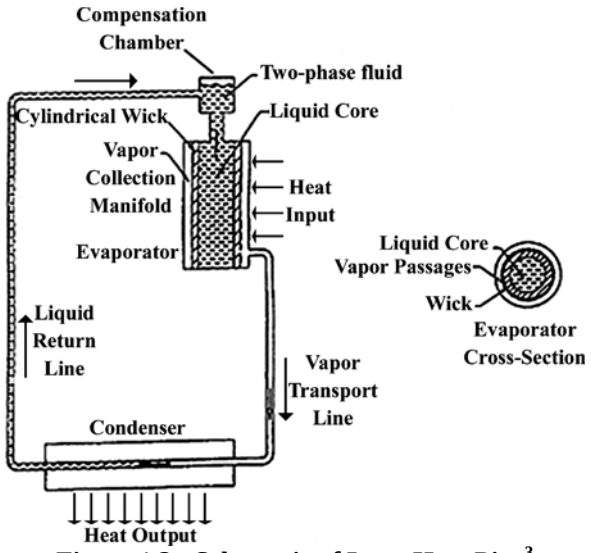

Figure 1.2 - Schematic of Loop Heat Pipe[3]

Both CPLs and LHPs are capable of dispersing heat quickly from a heat source and transporting it to remotely located heat sinks. A CPL provides tight temperature control, but requires a tedious and sometimes time consuming priming process prior to start-ups.[8] Conversely, a LHP can start, stop, and re-start at any time, but temperature control is not always possible.[8]

CHAPTER 2

DESIGN OF EXPERIMENTAL TEST APPARATUS

Results of earlier studies done by UAH, and others, on the Qu Tube pointed towards areas of the experimentation that needed to be improved, including performance aspects that deserved further study. Our planned testing of the Qu Tube therefore centered around several objectives. The first of these was to design and build a versatile test bed that could be used for future work. Part of this test bed would include the use of thermistors, rather than thermocouples, to improve accuracy and allow small temperature differences to be measured. The thermistors would need to be well calibrated in order to minimize the experimental uncertainty to the extent possible, and to help ensure a high confidence level for the data collected. By measuring small temperature differences determined from the thermistor measurements, our analysis indicated that the thermal conductivity for the Qu Tube could be determined if other conditions were met. The determination of the thermal conductivity was considered to be a major objective. Due to the high thermal conductivities demonstrated by Qu Tubes in earlier UAH tests, it was necessary for the new test bed to have a high heat rate capability, of the order of 5,000W, and be able to accommodate Qu Tubes of long lengths up to 10'. Also of importance was the ability of the test apparatus to rotate the long Qu Tubes so that any performance

changes with changes in tube inclination could be recorded. A final objective was to ascertain the axial heat flux.

Qu Tubes of a longer length were purchased with funds from an additional NASA grant. Nine Qu Tubes were purchased that were 10' in length and 5/16" in diameter. A tenth tube was purchased with the same dimensions, but was a plain copper tube of the same type used for the Qu Tubes. This was used as a control case. The Qu Tubes were tested in a new UAH experimental apparatus that rotated in order to test the tube at different angles with respect to gravity, was capable of 5000W input power, and had a calorimeter. Thermistors were used in the new system instead of thermocouples to improve accuracy of the temperature measurements. However, the thermistors had a lower operating temperature range than the thermocouples. To keep inside the "safe" temperature range required a balance between the input power into the Qu Tube and the flow rate of the calorimeter. Extended use outside of the operating range could have changed the thermistor elements' resistance as a function of temperature properties.

One tube was used to conduct initial checkout tests using a 150W electric band heater and free convective cooling. A nearly constant temperature, well within the uncertainty of the thermocouples, was measured along the tube, implying that the 10 foot tubes had a thermal conductivity at least 10,000 to 30,000 times higher than an equivalent plain copper tube. This lower bound of thermal conductivity was determined using a fin conduction analysis with free convective cooling in air. A curve was generated from a standard fin analysis for a copper tube 10' in length. The fin analysis used was verified by testing the plain copper 10' tube in the same setup. The copper thermal conductivity was multiplied by factors of 1,000 to 30,000 and the temperature gradient curves plotted.

The curve for 30,000 times the thermal conductivity of copper aligned best with the Qu Tube test data. Above this factor there was no observable change in the essentially constant temperature along the tube. A plot of typical results is shown in Figure 2.1. A draft technical note was written presenting the results of the checkout tests and is awaiting submittal to an AIAA journal. To our knowledge, no refereed journal articles have been published regarding the Qu Tube, and reports available from other resources are very limited. There was also no source of consistent information from the manufacturer. This lack of information significantly hindered the understanding of the behavior of the Qu Tube, and also led to some concerns in the heat transfer community that the "solid state" effect was not real. It was therefore imperative that UAH have a well-characterized and well-calibrated test apparatus to legitimately assess the Qu Tube's properties.

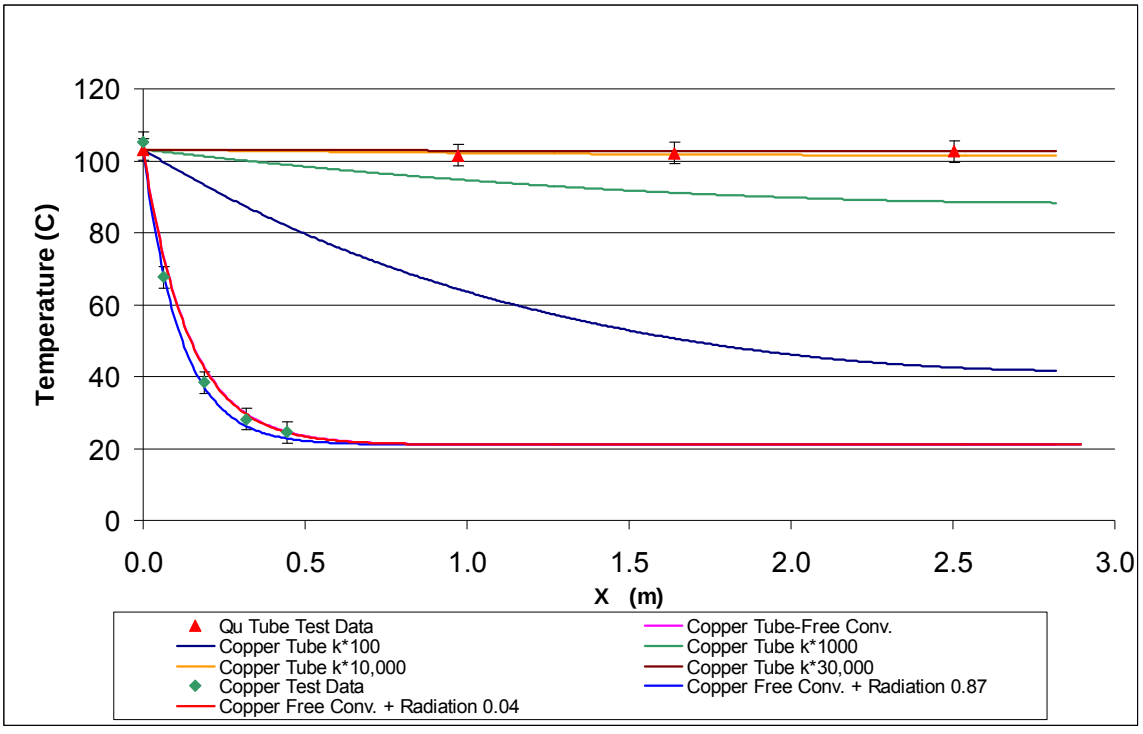

Figure 2.1 - T(x) for a Copper Tube Fin Compared with Experimental Data

2.1 Experiment Rationale

Quantifying the behavior of the Qu Tube, and assessing the various anomalous behaviors reported by others, required the design of a practical, versatile, well-calibrated test apparatus that enabled valid data to be collected. Previous exploratory tests and reported results aided in developing the requirements for such an apparatus.

The initial primary objective was to assess thermal conductivity and heat flux, since these were the main properties of importance for applications. Previous attempts to experimentally quantify the thermal conductivity of Qu Tubes yielded mixed results due to the tube being essentially isothermal along its length. The differences in temperature that the K-type thermocouples measured were not greater than that of the error of the thermocouples, ± 3ºC. By switching to properly calibrated thermistors the measurement error of the thermistors themselves was reduced to ± 0.1ºC. There was a small variation in the thermistor temperature measurement due to such effects as the area in contact with the surface of the tube, a temperature gradient across the thermistor, and repeated handling of the elements. It was therefore necessary to consider these aspects as well.

By having longer tubes and higher heat rates than with previous tests, temperature differences along the tube could presumably be accurately measured even if the effective thermal conductivity was 30,000 times that of copper. Therefore, knowing the heat rate, temperature difference, and tube cross-sectional area, a thermal conductivity could be calculated. The test apparatus would need to be able to test tubes that were 10 feet in length, be able to rotate to characterize performance at different angles of inclination, have an input heat rate of tens of watts up to 6,000W, be well insulated, have an instrumented calorimeter to remove the heat, ensure the same contact resistance for

each thermistor, use a versatile data acquisition system, and have accurate instrumentation capable of capturing small differences in temperature along the heat pipe.

2.2 Approach

The design for the new experimental apparatus began with the requirement that a 10’ tube needed to be rotated from the horizontal to near vertical in both directions. To accomplish this, a wooden A-frame was constructed with a 2” diameter axle placed near the top. The test article was mounted to a 2” x 10’ board that was attached to the axle using a U-bolt. A picture of the apparatus with the heater package and an un-insulated calorimeter is shown in Figure 2.2. Measurement of the angle of the tube in the apparatus was done using a digital protractor, shown in Figure 2.3.

Figure 2.2 - Rotatable Heat Pipe Experimental Apparatus

Figure 2.3 - Digital Protractor Used to Measure the Angle of the Test Article

2.2.1 High Heat Flux

Another design consideration was the need to have a temperature gradient along the length of the tube to calculate thermal conductivity. Using a thermal conductivity of 30,000 times that of copper (380 W/m-K), estimated from data in Figure 2.1, a heat rate of 6000W was found to produce a temperature gradient of 10ºC over a length of 1 meter. In order to put 6kW into the Qu Tube, coil heaters rated at 2kW each were purchased, and are shown in Figure 2.4. Each coil heater has an inner diameter of 1" and a length of 7". In order to adapt the coil heaters to the 5/16" outer diameter of the Qu Tube, a 1" diameter copper bar was cut into 7" sections (the same length as a single coil heater) and then a 21/64" hole was drilled down the center. A smaller hole was drilled just beneath the outer surface of the bar, and a similar hole was drilled next to the outer diameter of the hole drilled down the center. These two smaller holes, shown in Figure 2.5, allowed for the placement of thermocouples that would measure the radial temperature gradient through the copper bar. A high temperature thermal grease (AOS Heat Sink Compound 52027 XT) was used at the copper bar and test item interface. The purpose of the grease was to increase the conduction of heat into the article being tested and make the removal of the heaters easier. A 3-phase power controller was used to power the coil heaters, which were wired in a Δ-configuration, shown in Figure 2.6. The power controller and fuses were placed inside a metal enclosure along with a Wattnode power meter (Type WNA-1P-240-P-193-TTL), Figure 2.7. A PID controller was used to adjust the power controller, and is shown in Figure 2.8 next to the metal enclosure.

Figure 2.4 - 2kW Coil Heaters

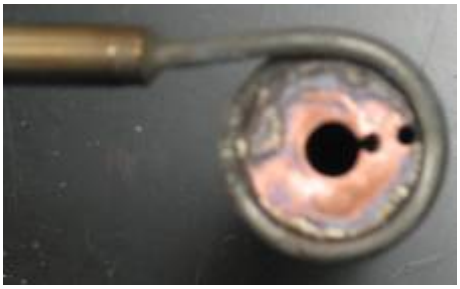

Figure 2.5 - Copper Bar with Two Thermocouple Holes

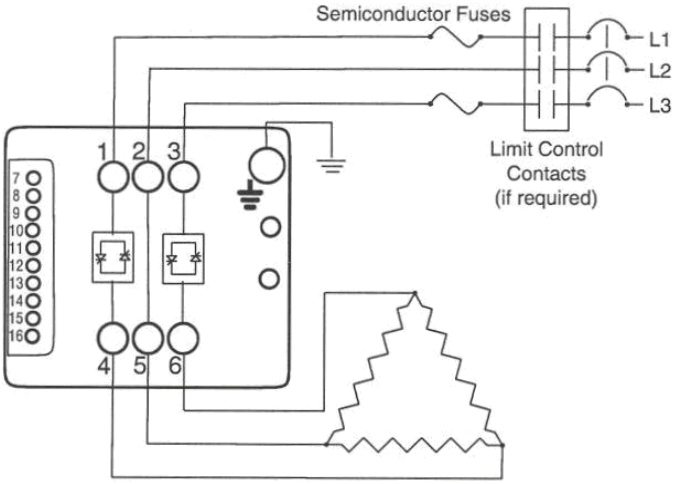

Figure 2.6 - 3-Phase Power Controller and Diagram of Coil Heaters Wired in a Delta Configuration

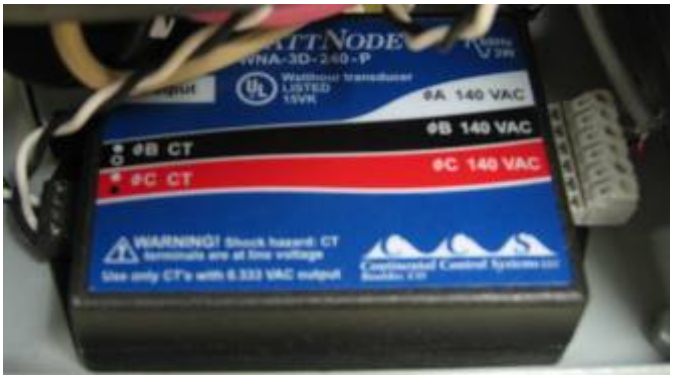

Figure 2.7 - Wattnode Power Meter Inside Enclosure

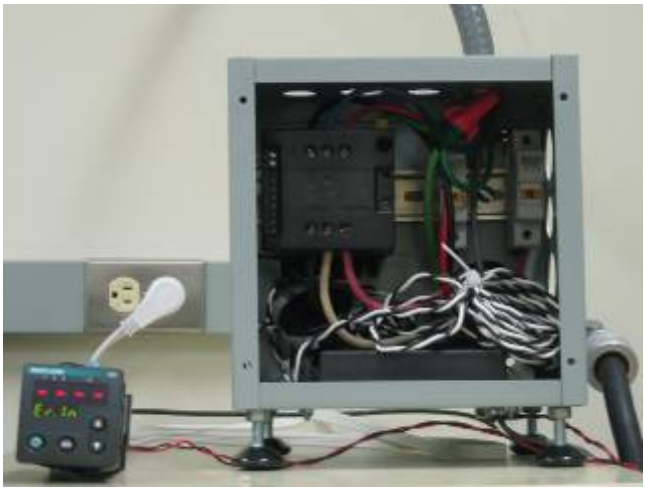

Figure 2.8 - Enclosure Containing Power Controller Next to PID Controller

2.2.2 Low Heat Flux

Testing the Qu Tube at lower power levels required the use of three variable AC power transformers, one for each coil heater. These variable transformers allowed greater control over the power at lower levels than the 3-phase power controller. Each transformer was accompanied by a power meter, shown in Figure 2.9, used for measuring the power used by an individual coil heater. For even lower power levels a DC power supply (Tenma 72-6610), shown in Figure 2.10, was used in conjunction with just one of the coil heaters. This was the power supply that was used for the thermistor qualification tests using a copper rod and a copper tube.

Figure 2.9 - Three AC Variable Transformers with Power Meters

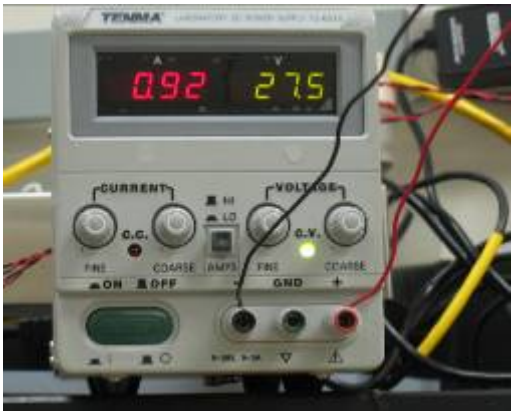

Figure 2.10 - DC Power Supply Used for Low Power Tests

2.2.3 Heater Insulation

Two types of insulation were used to insulate the heaters. The first type was a 1" thick high-temperature mineral wool cut to the length of a single coil heater, shown in Figure 2.11. This insulation was in direct contact with the heater coil. A custom made insulation jacket, purchased from Fabric Products Inc, was then wrapped around the mineral wool as shown in Figure 2.12. An illustration of the cross section of the heater coil and insulation is shown in Figure 2.13.

Figure 2.11 - Mineral Wool Insulation

Figure 2.12 - Custom Insulation Jacket Wrapped Around Mineral Wool and Coil Heater

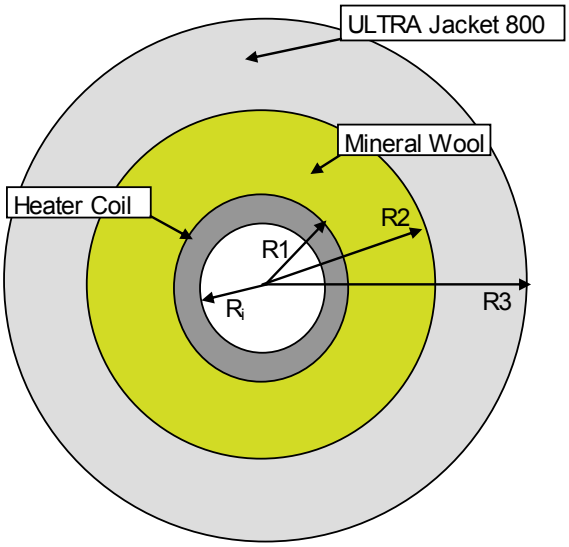

Figure 2.13 – Cross Section of Heater Coil and Insulation

2.2.4 Calorimeter

Heat was removed from the Qu Tube using a water calorimeter made from CPVC pipe and pipe fittings. The calorimeter is shown in Figure 2.14 without insulation. The calorimeter is approximately 3 feet in length with an inner diameter of 2". Before the water entered the calorimeter, it first flowed through a filter, pressure regulator, and a flowmeter. The pressure regulator maintained a nearly constant flow rate as the main water supply for the building varied during the day. From there the water flowed through a static mixer and past a thermistor probe, as shown in Figure 2.15. The water flowed over three sections of hand fabricated copper fins. Each section was 1' in length and had eight individual fins 0.025" thick. As shown in Figure 2.16, the tips of the fins are curved. This was done to give greater clearance with the inside of the calorimeter and to create turbulence in the flow to discourage boiling and increase the heat transfer rate into the water. At the exit of the calorimeter is another static mixer followed by a second probe thermistor to measure the temperature of the out-flowing water. Foam pipe insulation was used to minimize heat transfer to the room from the calorimeter, shown in Figure 2.17.

Figure 2.14 - CPVC Calorimeter

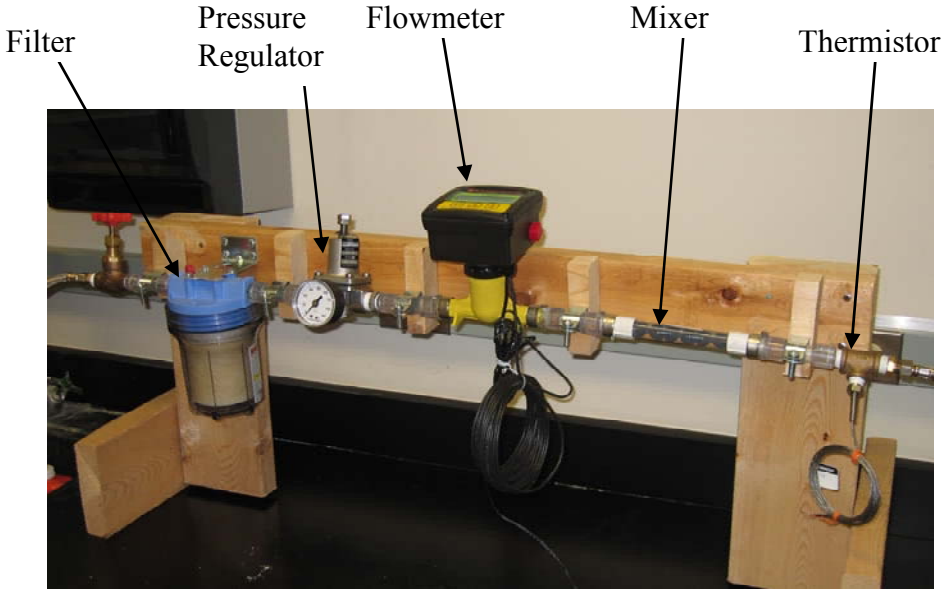

Figure 2.15 - Water Filter, Pressure Regulator, Flowmeter, and Thermistor Assembly

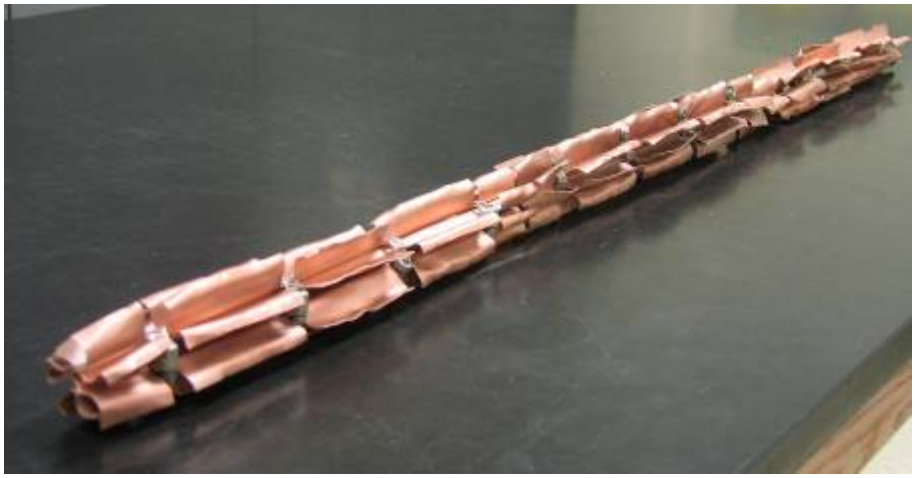

Figure 2.16 - Copper Fin Sections

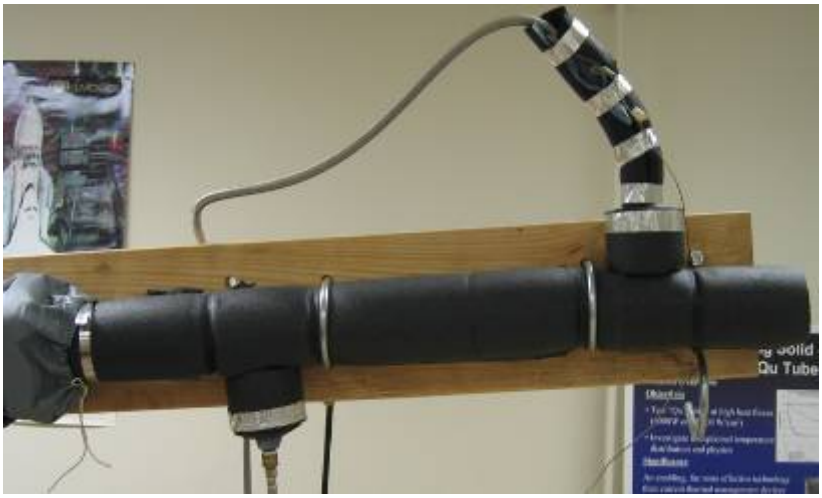

Figure 2.17 - Foam Insulated Calorimeter

2.2.5 Thermistor Rakes

In the early exploratory tests of the 18" Qu Tubes ensuring good contact between the thermocouples and the tube was a constant concern. Varying contact resistances between temperature sensors can cause an artificial temperature gradient. To solve this problem for the testing of the 10' Qu Tubes a thermistor rake was designed with spring-loaded Teflon pins to ensure constant pressure of the thermistors against the tube. Additionally, thermal grease (AOS Heat Sink Compound 52050-1 HTC 60) was also applied to the thermistors to minimize temperature gradients across the thermistors. An

analysis showed that having a thermal grease, with a thermal conductivity of 3.3 W/m K, instead of air in the thermistor gap, reduced the temperature difference between the tube surface and the thermistor to 0.145ºC. Since the active element of the thermistor was located essentially in the middle of the epoxy encapsulate, the expected temperature variation was likely even lower, perhaps on the order of 0.07°C. The analysis is covered in Section 2.3, and a cross section of the rakes and insulation is shown in Figure 2.18. The thermistor rakes were treated as cylinders rather than their actual geometry, which was rectangular, but this effect was relatively minor.

Each of the three rakes was 40 cm in length, with a height and width of 6.5 cm when the top and bottom halves were assembled together. Figure 2.19 shows a CAD drawing of the rake with the pin and spring. Semi-circular grooves were cut along the center-line to allow the thermistor wires to exit the rake, and can be seen in Figure 2.20. The grooves allow a short section of lead wire for the thermistor to see the same temperature as the element, thus minimizing conduction losses. A distance of 2 cm separates each groove. However, due to the limited number of data acquisition channels, the thermistors were placed 4 cm apart during experimentation. The rakes were made out of Delrin, an acetal resin engineering plastic. Delrin was chosen for its machine-ability and low thermal conductivity. A top half with a 5/16" groove, shown in Figure 2.21, was bolted to the bottom half as shown in Figure 2.22. To insulate the Delrin thermistor rakes, a custom insulation jacket was purchased, shown unwrapped in Figure 2.23.

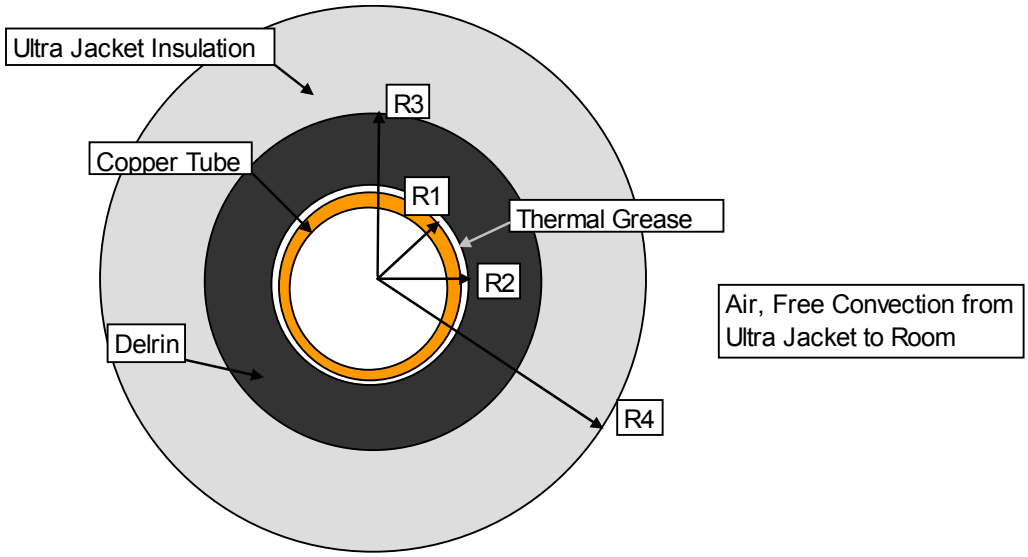

Figure 2.18 – Cross Section of Thermistor Rake and Insulation

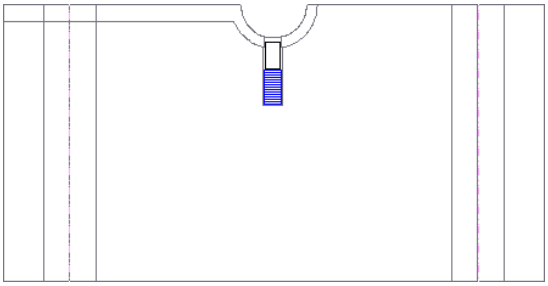

Figure 2.19 - Side View of Thermistor Rake CAD Drawing Showing Spring and Teflon Pin

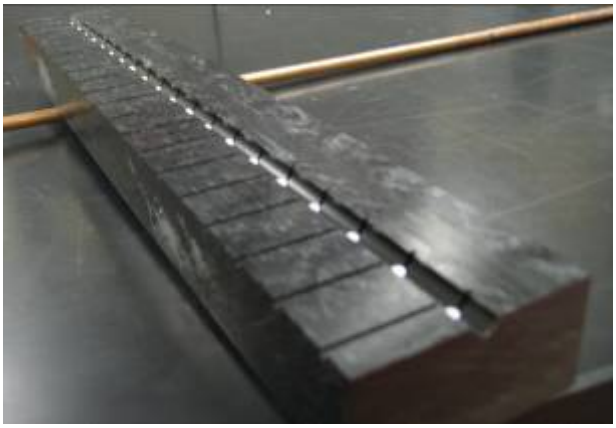

Figure 2.20 - Delrin Thermistor Rake Showing White Teflon Pins and Thermistor Grooves

Figure 2.21 - Top Half of Delrin Thermistor Rake

Figure 2.22 - Assembled Delrin Thermistor Rake with Thermistors

Figure 2.23 - Custom ULTRA Jacket Insulation for Delrin Thermistor Rakes (shown unwrapped)

2.2.6 Data Acquisition

Data acquisition was done using National Instruments LabVIEW 8 software and a National Instruments SCXI –1000 with a digitizer and USB output, shown in Figure 2.24. The SCXI-1000 had thirty-two channels for thermistors and was also used for eight thermocouple channels, voltage input from the flowmeter, and input from the WattNode powermeter. Also in the SCXI-1000 was a 100μA constant current source to power the thermistors. These inputs were then digitized and sent to the computer via a USB connection. From there the signals were organized and processed by the LabVIEW code shown in Figure 2.25. In this code the water flowrate, originally in gallons per minute, was converted to kg/s and multiplied by the difference in the water temperatures in and out of the calorimeter, and by the specific heat of water. This determined the amount of power taken out of the test article by the calorimeter using

$$q = \dot{m} c_P (T_{Out} - T_{In}) . \tag{2.1}$$

Temperature was calculated by taking the resistances of the thermistor elements and plugging them into the Steinhart and Hart Equation

$$\frac{1}{T} = A + B\ln(R) + C(\ln(R))^3 , \tag{2.2}$$

where A, B, and C are coefficients determined by the calibration data, and is discussed in Chapter 3. Data was taken at a rate of 200hz and then averaged by a factor of ten, and was executed once every minute for long duration tests.

The LabVIEW front panel, shown in Figure 2.26, consisted of two waveform charts, one for thermistors and the other for thermocouples. This was done to reduce the amount of data on one chart, but also because of the difference in temperature ranges that

the thermistors on the tube would be seeing (30 to 80°C), versus the thermocouples that were measuring heater temperatures that were at hundreds of degrees Celsius. Also on the front panel were individual temperature readouts for each thermistor and thermocouple, as well as power frequency, heater power, water flowrate in gallons per minute, and the amount of power removed by the calorimeter.

Figure 2.24 - National Instruments SCXI-1000 with Digitizer

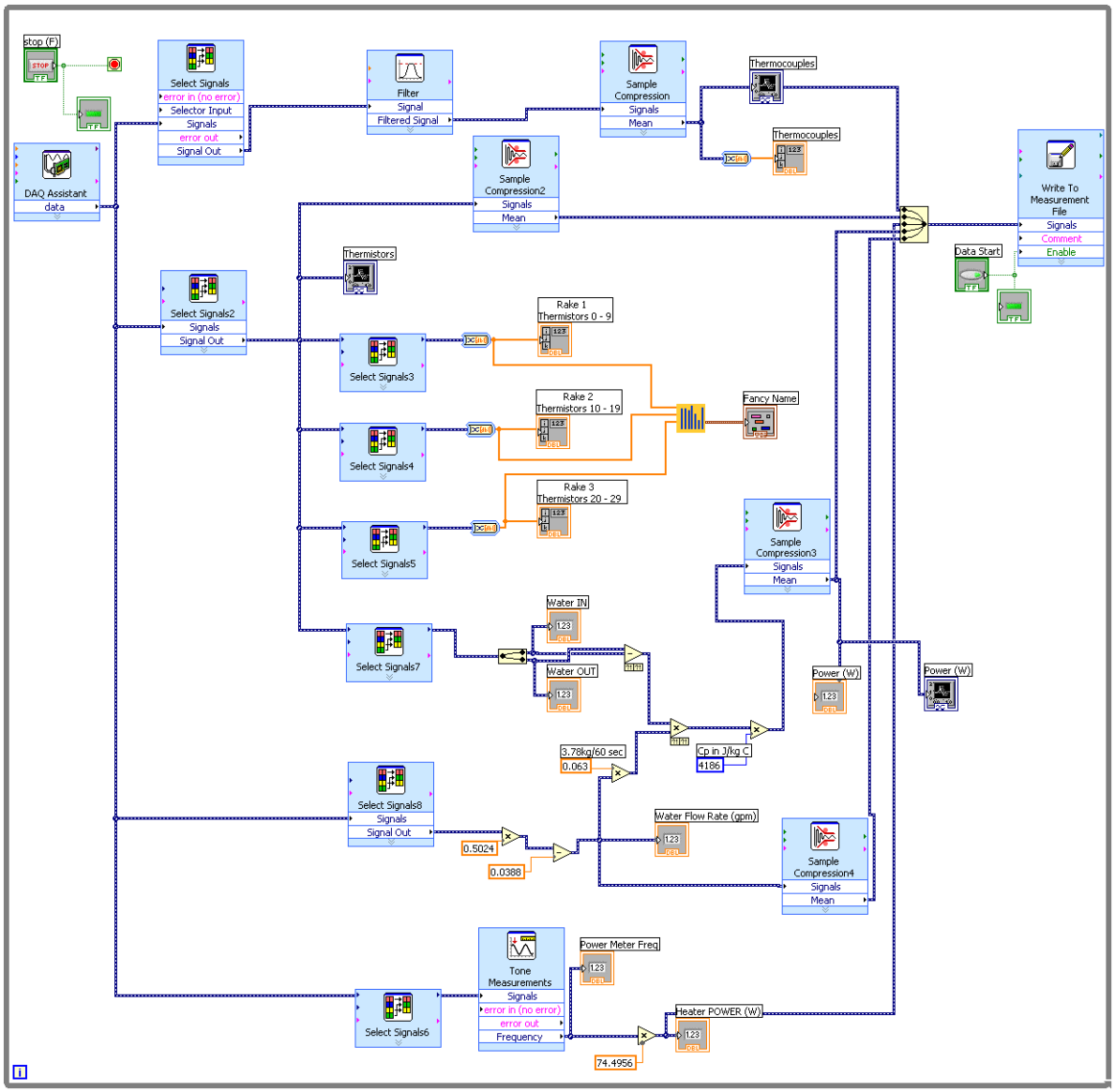

Figure 2.25 - LabVIEW 8 Block Diagram Code

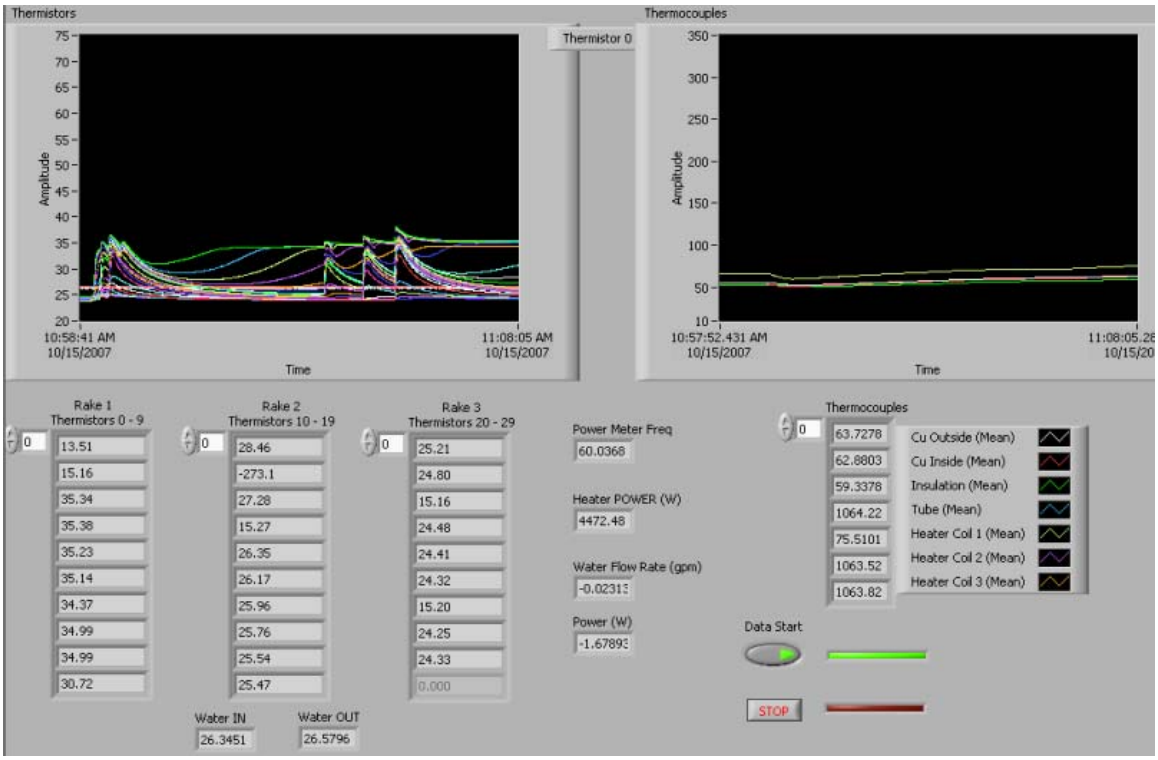

Figure 2.26 - LabVIEW Front Panel

2.2.7 Thermistors

Omega series 44032 thermistors with a resistance of 30,000 ohms at 25°C were used in the experimentation. Table 2.1 shows resistance versus temperature for the 44032 thermistor. Note that resistance decreases with an increase in temperature. The elements had a maximum diameter of 0.095" and two 3" lead wires, a drawing is shown in Figure 2.27. Each thermistor was soldered to 15' extension wires. The resistance of the lead wire extensions was calculated and then converted to an equivalent temperature difference to ensure that the length of the wires would not have an appreciable affect on the temperature measurement.

Table 2.1 - Resistance Versus Temperature for Omega Series 44032 Thermistor

RESISTANCE VERSUS TEMPERATURE – 40° to +100°

TEMP°C	RES	TEMP°C	RES	TEMP°C	RES	TEMP°C	RES	TEMP°C	RES
-40	884.6K	-10	158.0K	+20	37.30K	+50	10.97K	+80	3843
39	830.9K	9	150.0K	21	35.70K	51	10.57K	81	3720
38	780.8K	8	142.4K	22	34.17K	52	10.18K	82	3602
37	733.9K	7	135.2K	23	32.71K	53	9807	83	3489
36	690.2K	6	128.5K	24	31.32K	54	9450	84	3379
35	649.3K	5	122.1K	25	30.00K	55	9109	85	3273
34	611.0K	4	116.0K	26	28.74K	56	8781	86	3172
33	575.2K	3	110.3K	27	27.54K	57	8467	87	3073
32	541.7K	2	104.9K	28	26.40K	58	8166	88	2979
31	510.4K	-1	99.80K	29	25.31K	59	7876	89	2887
-30	481.0K	0	94.98K	+30	24.27K	+60	7599	+90	2799
29	453.5K	+1	90.41K	31	23.28K	61	7332	91	2714
28	427.7K	2	86.09K	32	22.33K	62	7076	92	2632
27	403.5K	3	81.99K	33	21.43K	63	6830	93	2552
26	380.9K	4	78.11K	34	20.57K	64	6594	94	2476
25	359.6K	5	74.44K	35	19.74K	65	6367	95	2402
24	339.6K	6	70.96K	36	18.96K	66	6149	96	2331
23	320.9K	7	67.66K	37	18.21K	67	5940	97	2262
22	303.3K	8	64.53K	38	17.49K	68	5738	98	2195
21	286.7K	9	61.56K	39	16.80K	69	5545	99	2131
-20	271.2K	+10	58.75K	+40	16.15K	+70	5359	+100	2069
19	256.5K	11	56.07K	41	15.52K	71	5180		
18	242.8K	12	53.54K	42	14.92K	72	5007		
17	229.8K	13	51.13K	43	14.35K	73	4842		
16	217.6K	14	48.84K	44	13.80K	74	4682		
15	206.2K	15	46.67K	45	13.28K	75	4529		
14	195.4K	16	44.60K	46	12.77K	76	4381		
13	185.2K	17	42.64K	47	12.29K	77	4239		
12	175.6K	18	40.77K	48	11.83K	78	4102		
11	166.6K	19	38.99K	49	11.39K	79	3970		

Figure 2.27 - Drawing of Omega Series 44032 Thermistor

2.3 Cylindrical Conduction Analysis

By treating each layer of insulation, or thermal grease, as a thermal resistance to the radial conduction of heat, an estimation of the amount of heat lost could be made. The experimental apparatus was divided into sections that were analyzed individually. The heat loss, q, of each section was determined using, for the case of three layers of insulation,

$$q = \frac{T_{\infty,1} - T_{\infty,4}}{\frac{1}{2\pi r_1 L h_1} + \frac{\ln(r_2/r_1)}{2\pi k_A L} + \frac{\ln(r_3/r_2)}{2\pi k_B L} + \frac{\ln(r_4/r_3)}{2\pi k_C L} + \frac{1}{2\pi r_4 L h_4}}. \quad (2.3)$$

When the heat losses from the different sections were summed, the total heat loss was 21.17 W, which compares very well with the 21.25 W heat rate from the power supply. The spreadsheet of the analysis is in Appendix B.

The results of the radial conduction analysis were also used to modify the design of the apparatus by identifying areas that were in need of more insulation. Also, the spreadsheet was used to compare the difference in heat transfer between the test article and the thermistor when air instead of thermal grease filled the gap.

CHAPTER 3

CALIBRATION AND UNCERTAINTY ANALYSIS

Traditional methods of determining thermal conductivity require a steady-state temperature difference over a certain length of a given cross-sectional area of well insulated material. Our earlier testing of Qu Tubes with thermocouples showed a nearly constant temperature along the tube with differences within the uncertainty of the thermocouples. Also, there are reports from tests conducted elsewhere that describe a sinusoidal temperature gradient along the tube with an amplitude of 1 to 2°C, Appendix A. In order to measure this unusual behavior and small differences in temperature along the length of the Qu Tube, the thermistors were calibrated using a specially designed copper calibration disk. Inside the disk the thermistors were equally spaced and symmetrically positioned. The resistance data from the calibration was used to generate coefficients and polynomial curve fits.

The temperature difference along the tube was the main focus of the experiment, not the absolute temperature, and therefore the thermistors were calibrated relative to one representative thermistor rather than an absolute standard. The disk was made out of copper alloy 101, also known as oxygen free high conductivity copper (OFHC), and was machined on a Haas CNC mill in the UAH Engineering Design & Prototyping Facility. The CNC machining of the copper calibration disk, which created

individual “wells” for each element and slots for the lead wires to exit the part, is shown in Figure 3.1 and Figure 3.2.

Figure 3.1 - Copper Calibration Part in CNC Mill

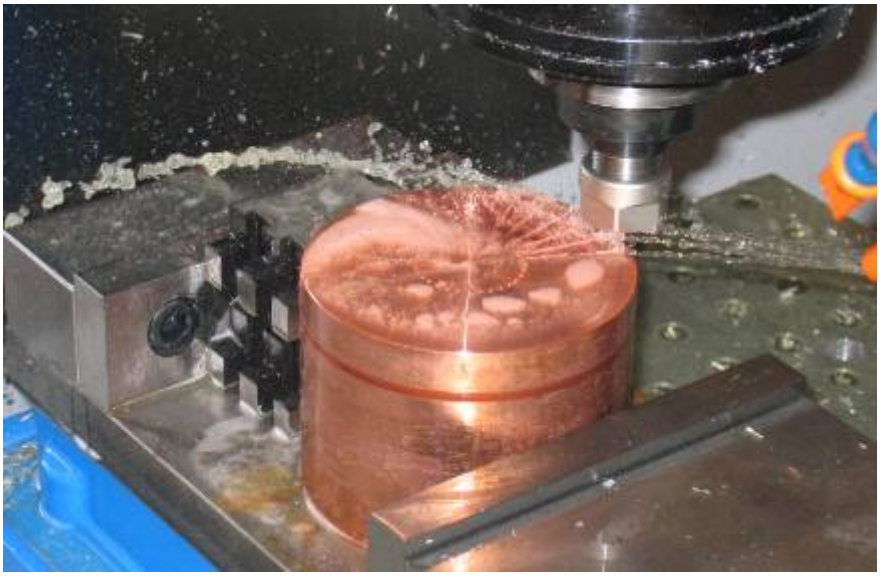

Figure 3.2 - Slots for Thermistor Wires Being Machined into Calibration Part

As shown in Figure 3.3, each thermistor was placed into the copper disk and the stress relieving ring, and each element covered in the AOS Heat Sink Compound 52050-1 HTC 60 thermal grease. The top to the copper disk is also shown, and was machined with teeth to ensure the top and bottom halves locked together.

Once the top was secured the part was wrapped in insulation and placed in a box made of foamboard insulation, shown in Figure 3.4. By having the thermistor elements in a tight circle, and very well insulated, it could be safely assumed that each thermistor was exposed to the same temperature. The box was then placed into a Tenney model T11RC Environmental Chamber that was set to 90°C. The thermistors soaked at this temperature for several days to ensure that a steady-state condition was reached. The oven was then turned off and the insulated thermistors were left inside to slowly cool. As the thermistors cooled, the resistance of each thermistor was data logged every 2 minutes, using the same data acquisition system to be used in the experimentation, generating the data shown in Figure 3.5.

Figure 3.3 - Thermistors in Copper Calibration Part with Thermal Grease

Figure 3.4 - Foamboard Box Containing Copper Calibration Part with Thermistors

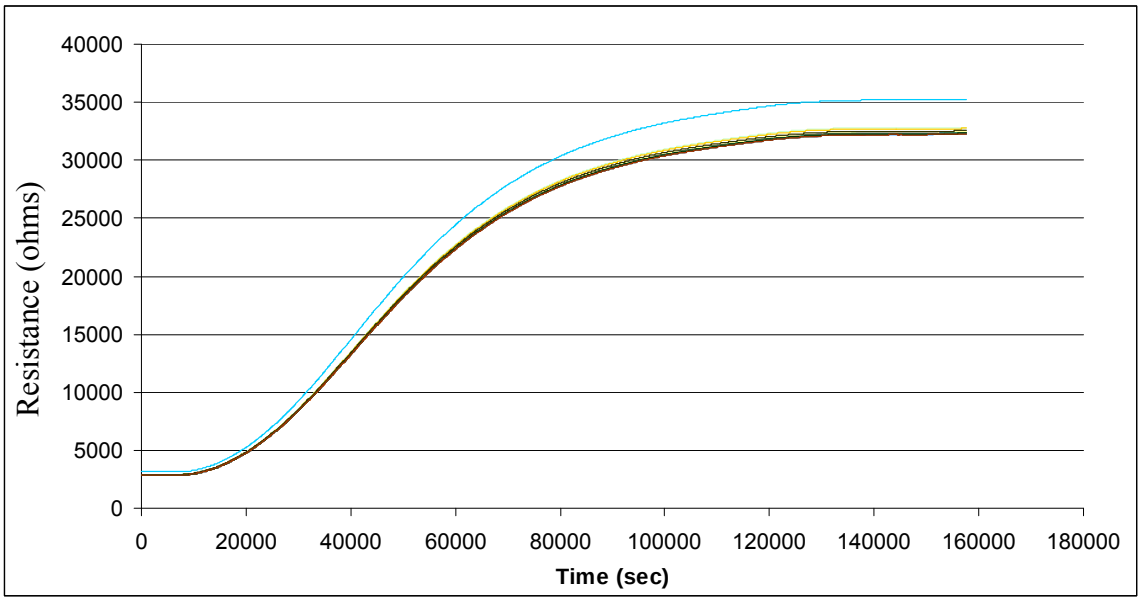

Figure 3.5 - Resistance vs. Time Collected During Calibration in Environmental Chamber

3.1 Generation of Individual Thermistor Coefficients

A thermistor was found that most closely matched the manufacture's values for resistance versus temperature in Table 2.1. This thermistor was then considered to be "the standard" to which the remaining thermistors were matched. Thermistor coefficients were generated using the Steinhart and Hart Equation,

$$\frac{1}{T} = A + B\ln(R) + C(\ln(R))^3, \tag{3.1}$$

where A, B, and C are coefficients determined using the resistances from the calibration data. In order to generate the coefficients, the resistance, R, for a single thermistor and a specific temperature, T, were plugged into Equation 3.1. By having the resistances for three specific temperatures, in this case 50, 70, and 90°C, it was possible to generate three Steinhart and Hart Equations with the three unknown coefficients. From these equations the A, B, and C coefficients for that particular thermistor were solved for and entered into LabVIEW.

3.2 Calibration Coefficients Checkout Tests

To check the validity of the coefficients, tests were conducted with a 5/16" diameter copper rod at room temperature. Data was collected using coefficients generated from the manufacture's data (every thermistor having the same coefficients), by using polynomial curve fits of the calibration data, and the coefficients generated by the calibration data. The results from these room temperature tests are shown in Figure 3.6. As can be seen in the figure, by using coefficients specific to each thermistor, instead of all of the thermistors using the same coefficients, a few outliers present in the data series were corrected. The average and standard deviation for each method is shown in Table 3.1. Having determined the best method of determining the thermistor coefficients, an uncertainty analysis was conducted to determine the systematic uncertainty.

Table 3.1 - Average and Standard Deviation for Each Method Used to Determine Thermistor Calibration

	Average (C)	Standard Deviation (C)
Coefficients from Calibration	24.143	0.093
All Coefficients the Same	24.007	0.388
Polynomial Curve Fit	23.724	0.182

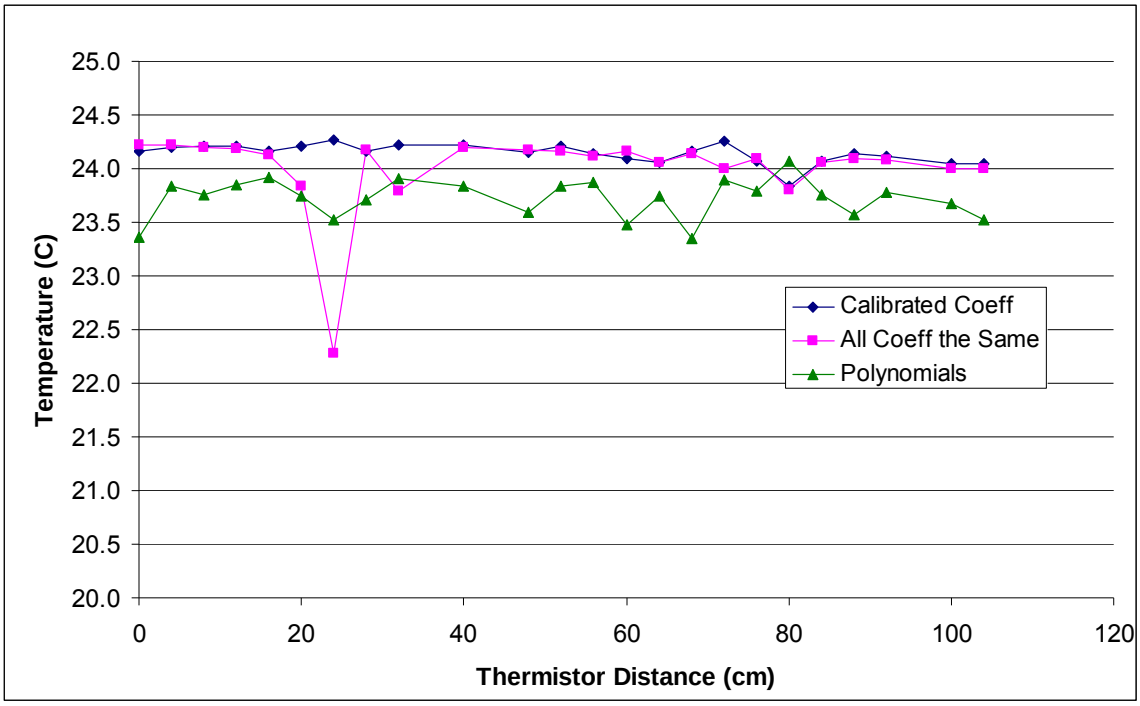

Figure 3.6 - Comparison of Different Thermistor Coefficient Methods

3.3 Uncertainty Analysis

The calibration setup and procedure were designed with the intent of eliminating the systematic errors between the readings of the thermistors, thereby reducing the systematic uncertainty. Systematic uncertainty is defined by Coleman and Steele as "the uncertainty component that arises from the effect of the systematic errors…"[9] However, some bias always remains as a result of calibration since no calibration procedure is perfect.[9] There are also potential biases due to "environmental and installation effects on

the transducer as well as the biases in the system that acquires, conditions, and stores the output of the transducer."[9]

Systematic uncertainty of the measurement is "calculated as the root-sum-square (RSS) of the elemental systematic uncertainties,"[9] $(B_i)_k$, using Equation 3.2

$$B_J = \left[\sum_{k=1}^{M} (B_i)_k^2 \right]^{1/2}. \tag{3.2}$$

Because the main objective of the experimentation was to measure temperature differences, no standard or reference thermistor was used. Therefore, there was not an elemental source of uncertainty associated with calibrating with a laboratory standard. It was also assumed that the copper disk used in the calibration had no spatial temperature non-uniformity, and so did not contribute an elemental source of uncertainty. This left the ± 0.1°C deviation of the thermistors as the only appreciable elemental source of uncertainty. Equation 3.2 became, for every thermistor,

$$B_T = \left[(0.1)^2 \right]^{1/2} = 0.1 . \tag{3.3}$$

The data reduction equation for this experimentation was

$$\Delta T = T_1 - T_2 \tag{3.4}$$

and the uncertainty analysis expression is

$$B_{\Delta T}^2 = \theta_{T_1}^2 B_{T_1}^2 + \theta_{T_2}^2 B_{T_2}^2 + 2\theta_{T_1}\theta_{T_2} B_{T_1 T_2} , \tag{3.5}$$

where

$$\theta_{T_1} = \frac{\partial \Delta T}{\partial T_1} = 1 \tag{3.6}$$

$$\theta_{T_2} = \frac{\partial \Delta T}{\partial T_2} = -1 . \tag{3.7}$$

In this case, because there were no elemental sources of uncertainty associated with a laboratory standard or spatial variation in temperature

$$B_{T_1 T_2} = 0 , \tag{3.8}$$

so that

$$B_{\Delta T}^2 = (1)^2 (0.1)^2 + (-1)^2 (0.1)^2 = 0.02 \tag{3.9}$$

or

$$B_{\Delta T} = 0.14^{\circ} C . \tag{3.10}$$

CHAPTER 4

TEST PROTOCOL

Once the test article was installed into the apparatus, as described in Appendix C, the insulation was removed to allow the use of the digital protractor to measure the angle of the tube. The angle of the board the tube was mounted to was then measured to determine the difference in angle between the two. The board was then rotated so that the test article was horizontal and the insulation was replaced. At this point LabVIEW was started, but not enabled to record data. Water flow was started and adjusted to the desired flowrate for the particular experiment to be conducted. The test article was then rotated back and forth to dislodge any air pockets in the calorimeter. A low power setting was used to start the experiment when testing items other than the Qu Tube. This was necessary so as to not exceed the maximum operating temperature of the thermal grease (350°C) and heater coils (650°C). The power was then slowly increased to the desired setting. Data recording was not needed at this point when testing the copper rod or tube, but the initial heating of the Qu Tube was recorded so that anomalous behavior could be documented if it occurred. Once the heater was at the power level designated for the test, the experiment was allowed to reach steady-state. LabVIEW was then enabled, and the steady-state condition was recorded for several hours, usually overnight, with the temperature recorded once every minute.

Next, the apparatus was rotated to the next angle to be tested. When testing the copper rod or copper tube the change in angle was straight forward. However, because the gravity-dependent Qu Tubes do not work at the -45° and horizontal settings, rotating the Qu Tube back to a positive angle causes the Qu Tube to very rapidly "activate," making the tube isothermal along its length. This rapid increase in temperature could potentially damage the thermistors or soften the Delrin. When running tests on the Qu Tube it was found to be beneficial to use a faster sampling rate when changing the angle, then switch to a slower rate when collecting steady-state data. Using a faster sampling rate under transient conditions enabled the capturing of unusual behavior in better detail.

CHAPTER 5

RESULTS AND DISCUSSION

Three test articles, a copper rod, copper tube, and a copper Qu Tube, were studied using the constructed apparatus and calibrated instrumentation. All three test items were tested at the same power level, flowrate, and angles of inclination. Also, every test item had the same external dimensions of 5/16" outer diameter and 10' in length.

An analysis of both a solid and annular cylindrical insulated fin was conducted in order to predict the expected results. The analysis was done for a fin with a length equal to the distance from the first thermistor to the last, 104 cm, with an outer diameter of 5/16". In the case of the annular fin, a wall thickness of 0.032" was used. Because the fin was insulated, an assumption was made that the convective heat loss from the tip was negligible, and therefore the fin tip could be treated as adiabatic. For this case, the temperature distribution for free convective heat loss is expressed as

$$\frac{\theta}{\theta_b} = \frac{\cosh m(L-x)}{\cosh mL} = \frac{T - T_\infty}{T_b - T_\infty}. \tag{5.1}$$

Solving Equation 5.1 for the fin temperature gives

$$T = T_\infty + \theta_b \left(\frac{\cosh m(L-x)}{\cosh mL} \right), \tag{5.2}$$

where m is calculated from m^2 using Equation 5.3

$$m^2 = \frac{UP}{kA_C}. \tag{5.3}$$

An equivalent area was used in the determination of the perimeter, P, by using the surface area. The equivalent area was then divided by the length to determine the perimeter. In order to account for the layers of material between the surface of the fin and the ambient surroundings, shown in Figure 5.1, an equivalent heat transfer coefficient was determined using Equation 5.4 from radial conduction through a cylindrical wall

$$U_{eq} = \frac{1}{\frac{r_1}{k_A}\ln\frac{r_2}{r_1} + \frac{r_1}{k_B}\ln\frac{r_3}{r_2} + \frac{r_1}{k_C}\ln\frac{r_4}{r_3} + \frac{r_1}{r_4}\frac{1}{h_4}}. \tag{5.4}$$

The spreadsheet used for this analysis is shown in Appendix D. As can be seen by the illustrations of the cross sections in the spreadsheet, the Delrin rakes were treated as being cylindrical in shape rather than rectangular. Results plotted with experimental data for the solid copper fin and annular copper fin are shown in Figure 5.2 and Figure 5.3 respectively. As can be seen in Figure 5.2, there was relatively good agreement between the predicted gradient for the copper rod and the gradient measured by the thermistors. The slight discrepancy between the experimental data and the analytical results is most likely because of the Delrin rakes being rectangular in shape instead of cylindrical. Figure 5.3 shows no distinguishable difference in the gradients for the insulated and uninsulated cases for the copper tube. The results also show the experimental data agreeing very well with the analysis for the insulated case.

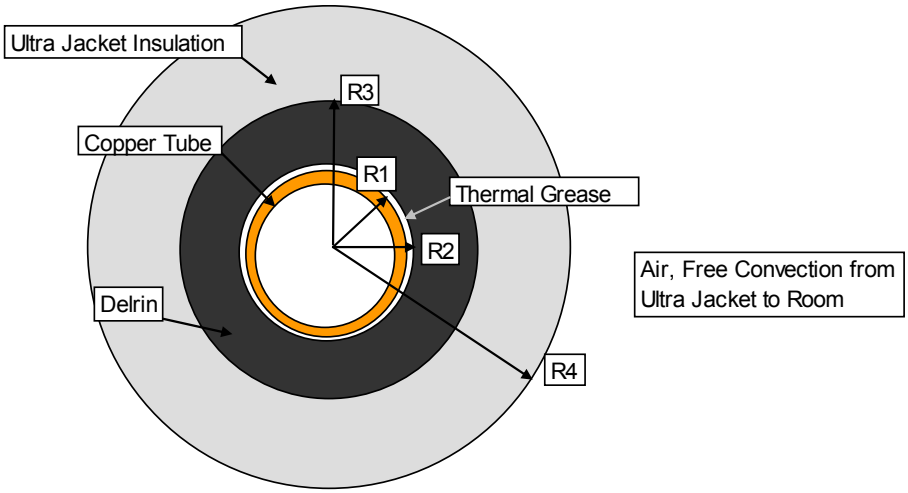

Figure 5.1 - Cross Section of Insulated Annular Fin Used in Analysis

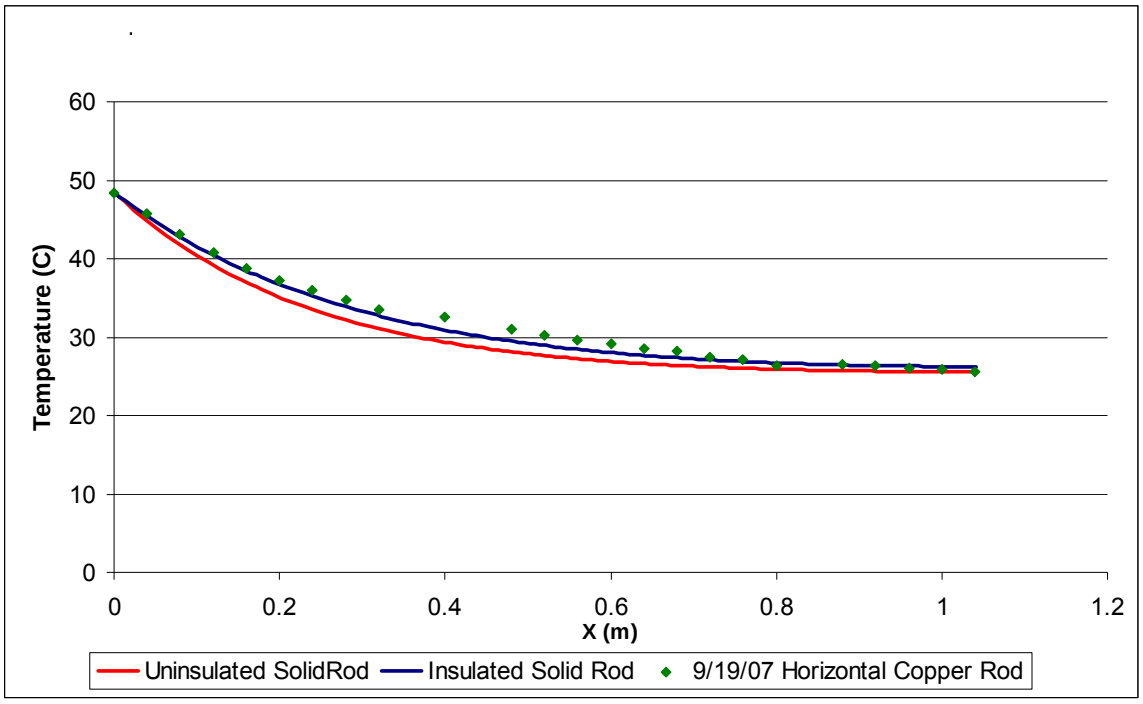

Figure 5.2 - Results of Insulated and Uninsulated Solid Rod Fin Analysis with Experimental Data

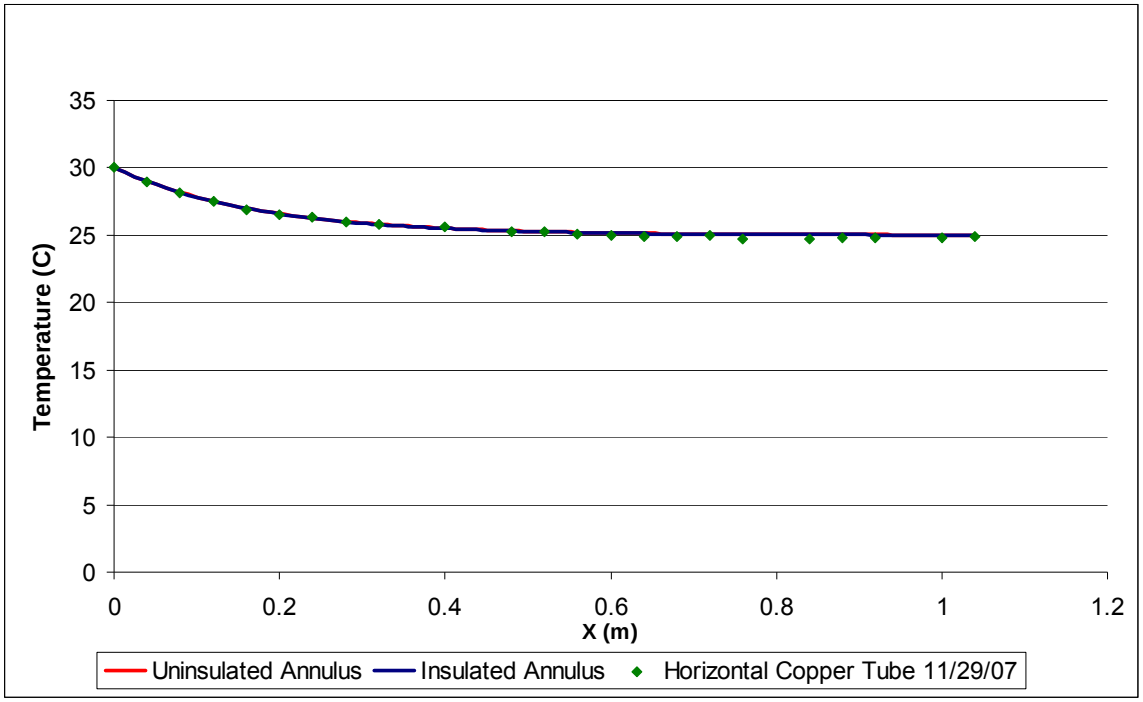

Figure 5.3 - Results of Insulated and Uninsulated Annular Fin Analysis with Experimental Data

5.1 Copper Rod

Before testing the Qu Tube it was necessary to ensure that the instrumentation was well behaved while the apparatus was both horizontal and in inclined positions. To do this, the first article to be tested was a solid copper rod 5/16" in diameter and 10 ft in length. A copper rod has predictable behavior and would not have internal convection like a copper tube. Therefore, if any unusual temperatures were measured while at steady-state or while changing the angle, it could be safely assumed that it was due to instrumentation. The power level at which the testing was conducted was determined by increasing the power level until the single coil heater being used to heat the horizontal copper rod reached a temperature of 300°C at the internal heater coil thermocouple. This power level was 21.25W DC. Once the horizontal copper rod had reached a steady-state condition, the apparatus was rotated to a +45° angle. For all tests conducted, a

+45° angle corresponded to the test item being heated from the bottom and cooled from the top. After steady-state data had been collected, the copper rod was then rotated to a -45° angle. Again, once the rod had reached steady-state the apparatus was rotated back to a horizontal position and the power was turned off. After the rod cooled and reached room temperature, the power was turned on and the preceding procedure was repeated to test for repeatability of the temperature measurements. The data from these tests were plotted as difference in thermistor n and thermistor n+1 temperature, divided by the distance between thermistors, versus the temperature difference location. The temperatures were divided by the distance between the thermistors because broken thermistors caused the distance between some thermistors to be greater than the standard 4 cm. Figure 5.4 shows the data for the tests conducted on the horizontal copper rod. As can be seen, there is excellent repeatability between the three tests. There is also definite repeatability in the results for the tests conducted at +45° and -45°, Figure 5.5 and Figure 5.6 respectively. Although the temperature differences between the thermistors stayed constant between the tests, there was a change in overall temperature noticed when the apparatus was rotated; this is shown in Figure 5.7. When the apparatus was rotated to the -45° position, the rod cooled down, indicating a loss of heat. Insulation was added to the back of the heater bundle, and also to the thermistor rake insulation. The copper rod was then retested at the same angles. Figure 5.8 shows how the added insulation reduced the change in temperature, but did not completely eliminate it.

By testing the copper rod at a constant power level, different angles, and obtaining repeatable results after angle changes showed that the instrumentation could be trusted. A copper tube was tested under the same conditions to see how the thermistors

measured a surface temperature with internal convection, and to collect data that could be used as a direct comparison to the Qu Tube data.

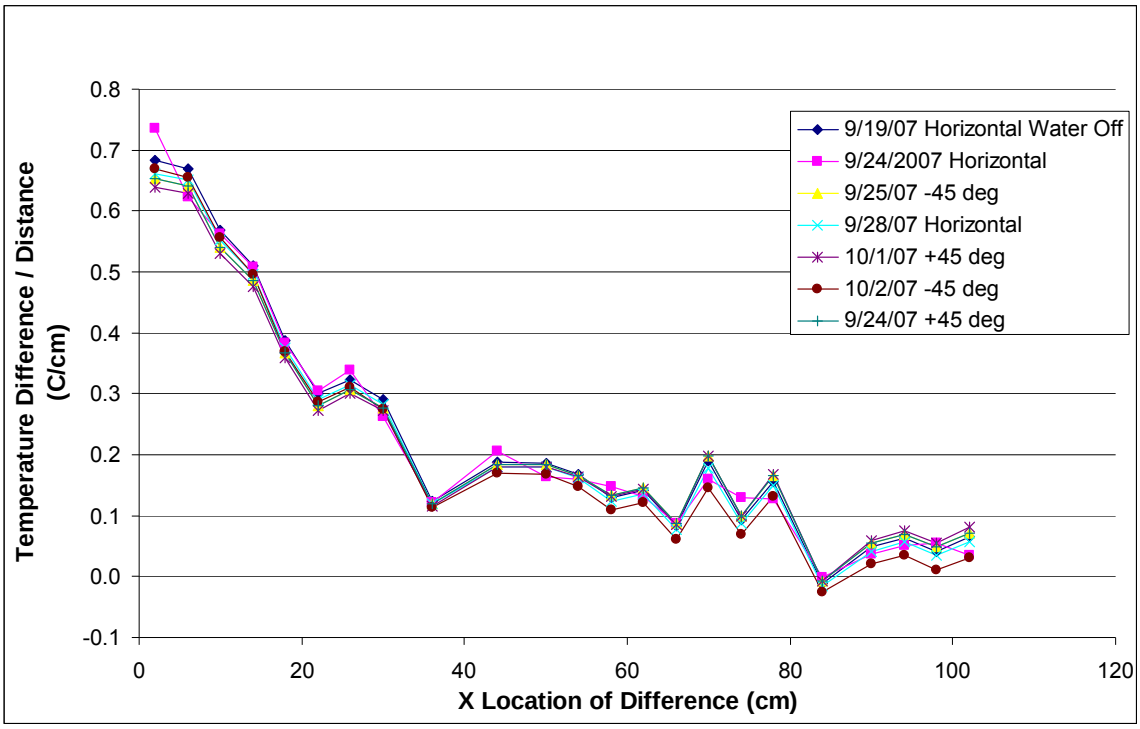

Figure 5.4 - Data for Horizontal Copper Rod

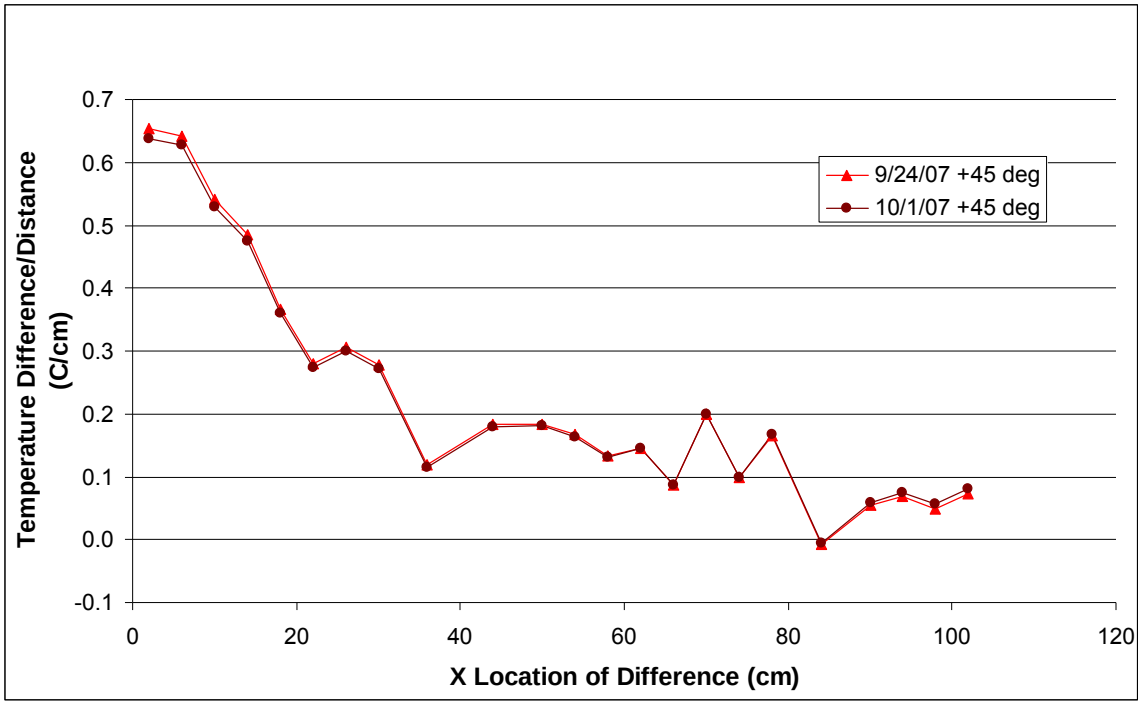

Figure 5.5 - Data for Copper Rod at +45 degree Inclination

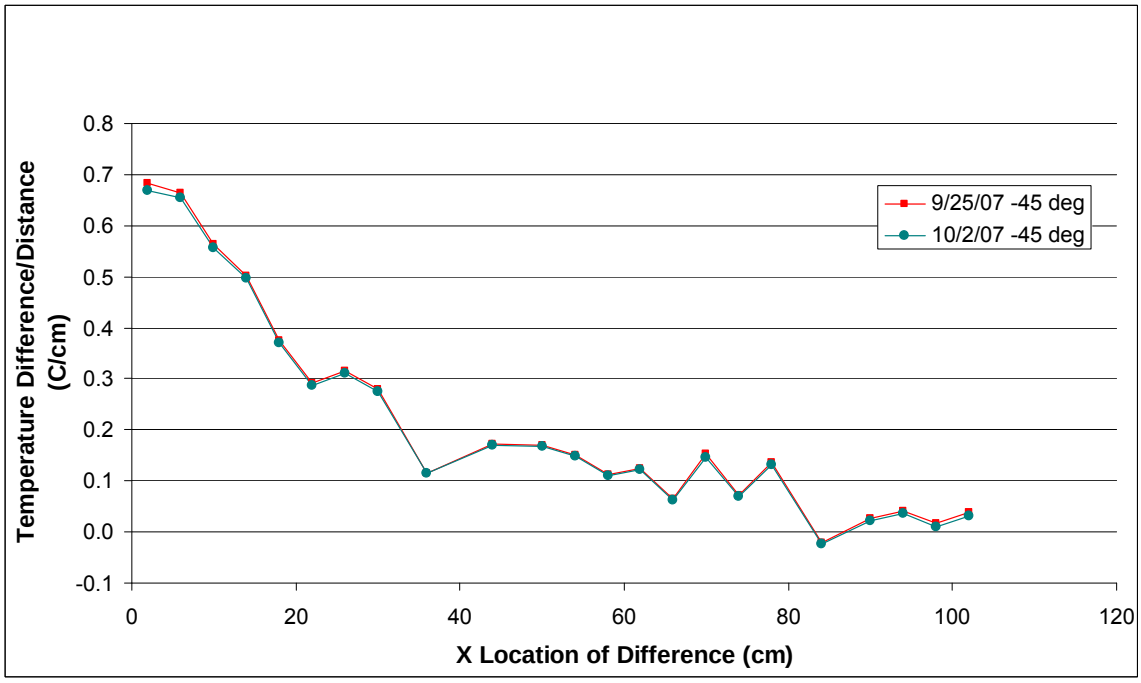

Figure 5.6 - Data for Copper Rod at -45 degree Inclination

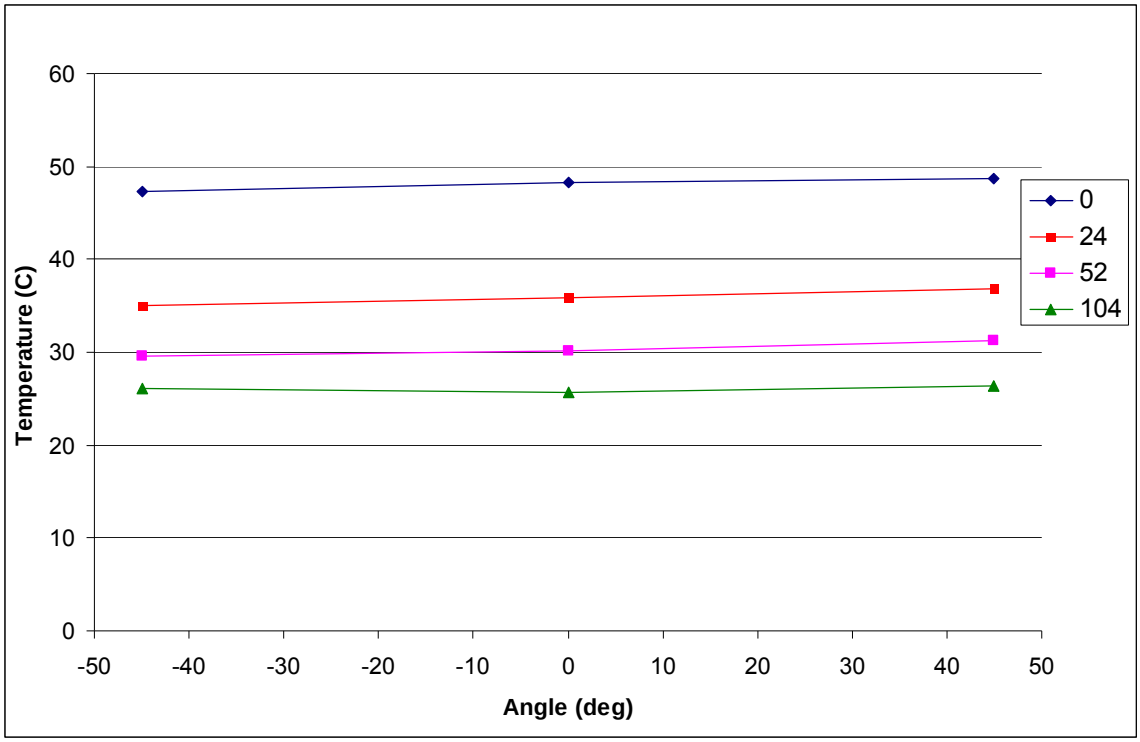

Figure 5.7 - Thermistor Temperature vs. Angle for Copper Rod

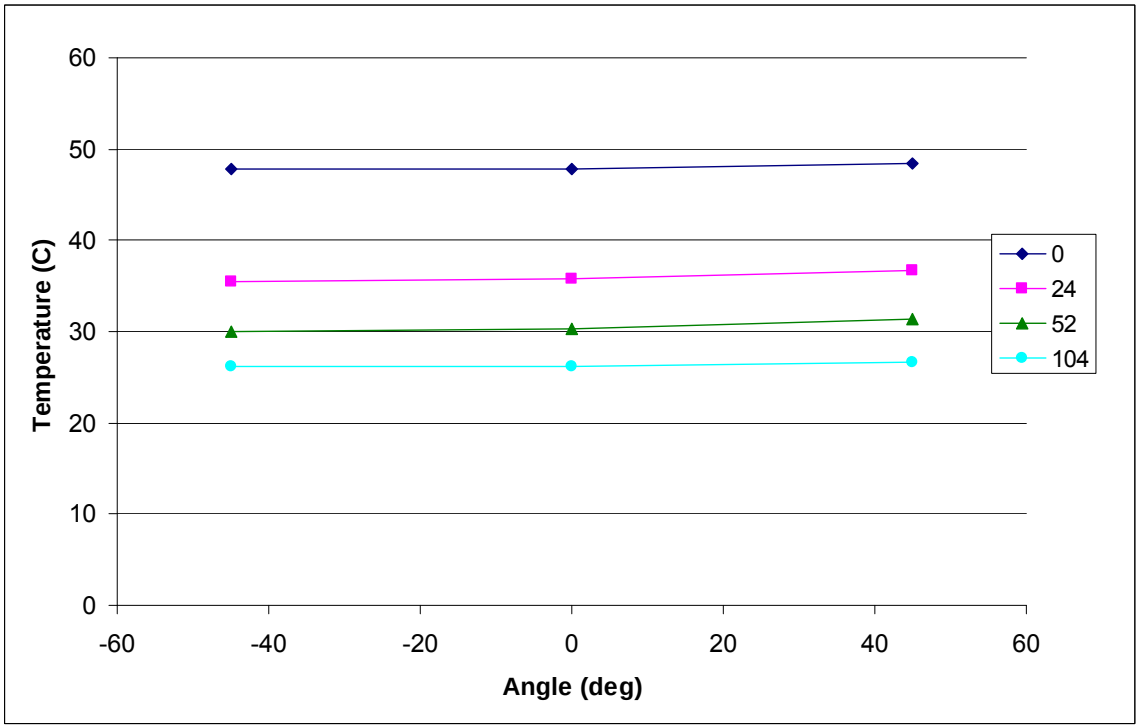

Figure 5.8 – Thermistor Temperature vs. Angle for Copper Rod with Added Insulation

5.2 Copper Tube

Results for the copper tube tested were plotted in the same manner as the copper rod data. As can be seen in Figure 5.9, there is excellent agreement between the three tests conducted. By having a high level of repeatability for the different test orientations, it was shown that any unusual temperature readings seen on the Qu Tube at different inclinations were a result of the Qu Tube's heat transfer mechanism, and not the result of the thermistors being rotated.

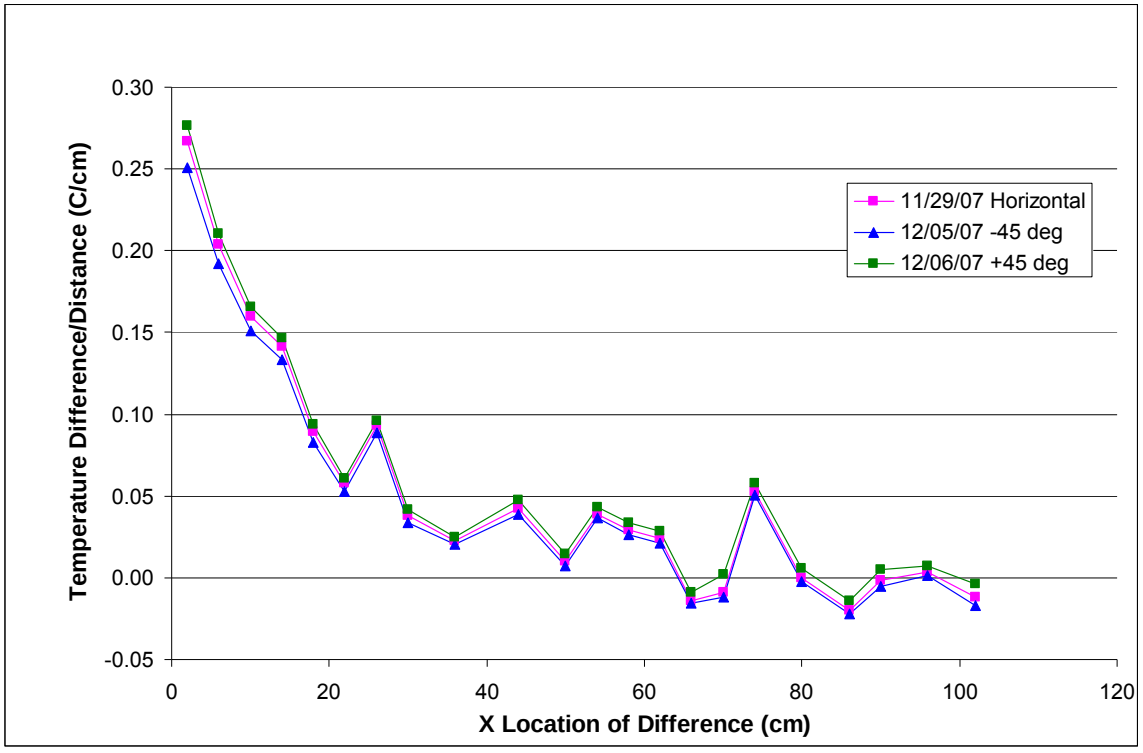

Figure 5.9 - Results for Copper Tube

5.3 Qu Tube

The Qu Tube was tested at the same conditions as the copper rod and copper tube, and using the same test procedure. Results showing temperature averaged over a period of steady-state condition, versus the x location of each thermistor are in Figure 5.10.

The Qu Tube was expected to behave like a copper tube when oriented at or below the horizontal. These expectations were confirmed when the Qu Tube was tested in the horizontal and -45° positions, shown in Figure 5.11 and Figure 5.12 respectively, and compared with the results from the testing of the copper tube, shown in Figure 5.14 and Figure 5.15. When the 10' Qu Tubes were ordered, the manufacturer stated that a gravity independent formula was not currently available in tubes that long in length, and would take more time to develop and cost much more to provide. Therefore, Qu Tubes that were gravity dependent were purchased. This gravity dependence explains the extreme change in the performance of the Qu Tubes when tested at different angles.

At an angle of +45º, the Qu Tube repeatedly had an essentially constant temperature along the length of the tube for the heat rates tested. This is illustrated in Figure 5.10 and Figure 5.13.

A test was also conducted with a Qu Tube utilizing all three coil heaters and a heat rate of 500W. The Qu Tube was at an angle of +45º and the water flow rate was 0.3 gpm. As with the test conducted with lower heat rate, the temperature along the sections measured by thermistors was essentially constant, as shown in Figure 5.16. With this heat rate and calorimeter flowrate, the power out of the Qu Tube was calculated to be 321.7W by averaging the data over a steady-state period of time, shown in Figure 5.17. Dividing the power out of the tube by the total outer cross-sectional area of the Qu Tube, 0.495 cm^2, gives a heat flux of 650 W/cm^2. During this test it became evident that there was a radial thermal resistance impeding heat from reaching the presumed heat transfer mechanism inside the tube. This internal radial thermal resistance was not known at the

time this study was initiated and is a potential problem that could limit Qu Tube applications; this effect deserves further study.

All Qu Tube results collected in this study have not shown any appreciable gradient in temperature with which to calculate the thermal conductivity. A temperature along the tube could be used, in principle, to estimate the effective thermal conductivity of the tube, knowing the heat rate, in watts, tube cross sectional area, and the gradient. However, the temperature gradients measured were essentially flat, and in some cases, even showed a slight increase in temperature relative to that near the heated end. An example of this is shown in Figure 5.10. Therefore, the data obtained to date does not allow an effective thermal conductivity to be estimated. This may require higher heat rates for the relatively high performance tubes we tested. Therefore, the thermal conductivity can still only be estimated as a lower bound using the approach shown in Figure 2.1.

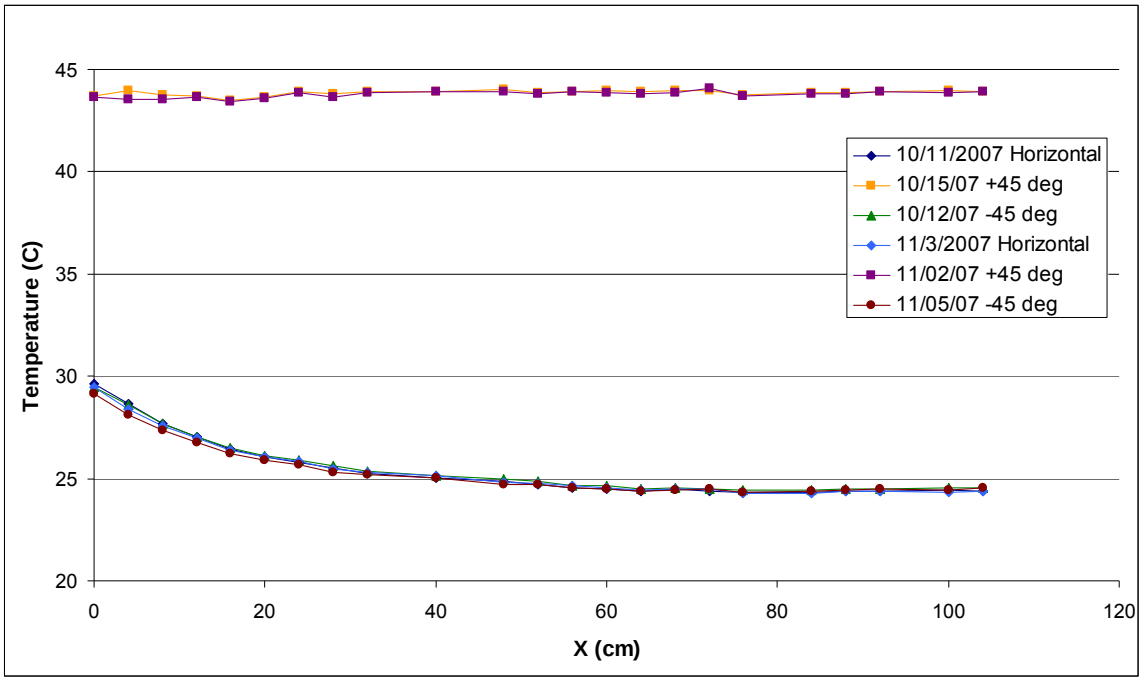

Figure 5.10 - Averaged T(x) for Qu Tube at Three Test Positions with Constant Power

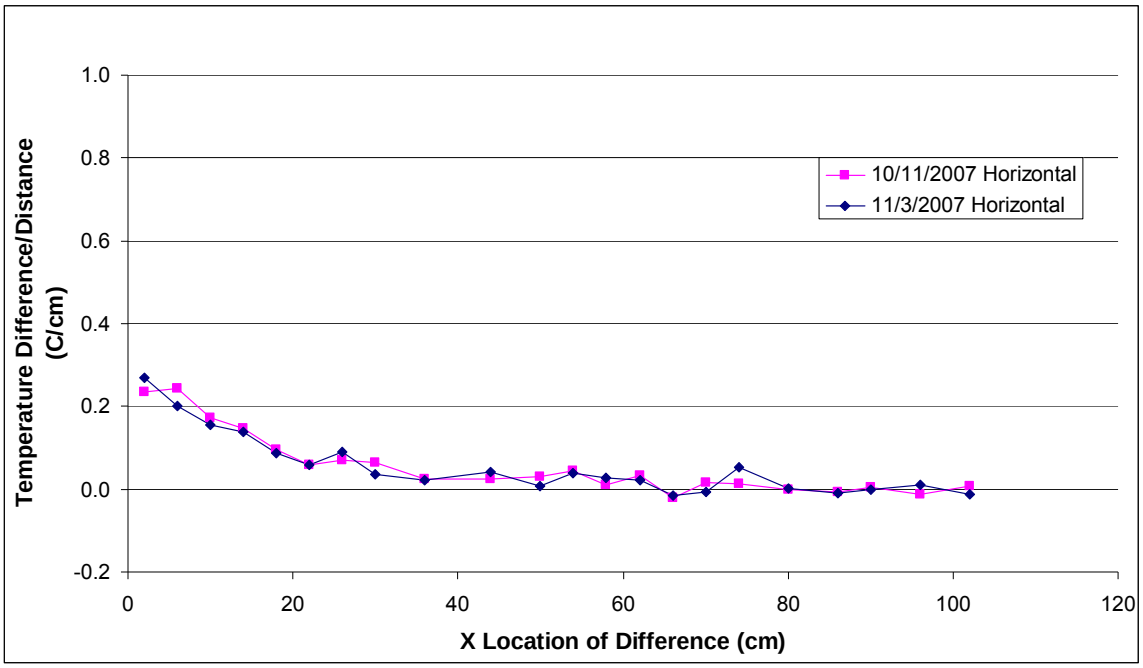

Figure 5.11 - Difference in Horizontal Qu Tube Temperature Divided by Distance Between Thermistors

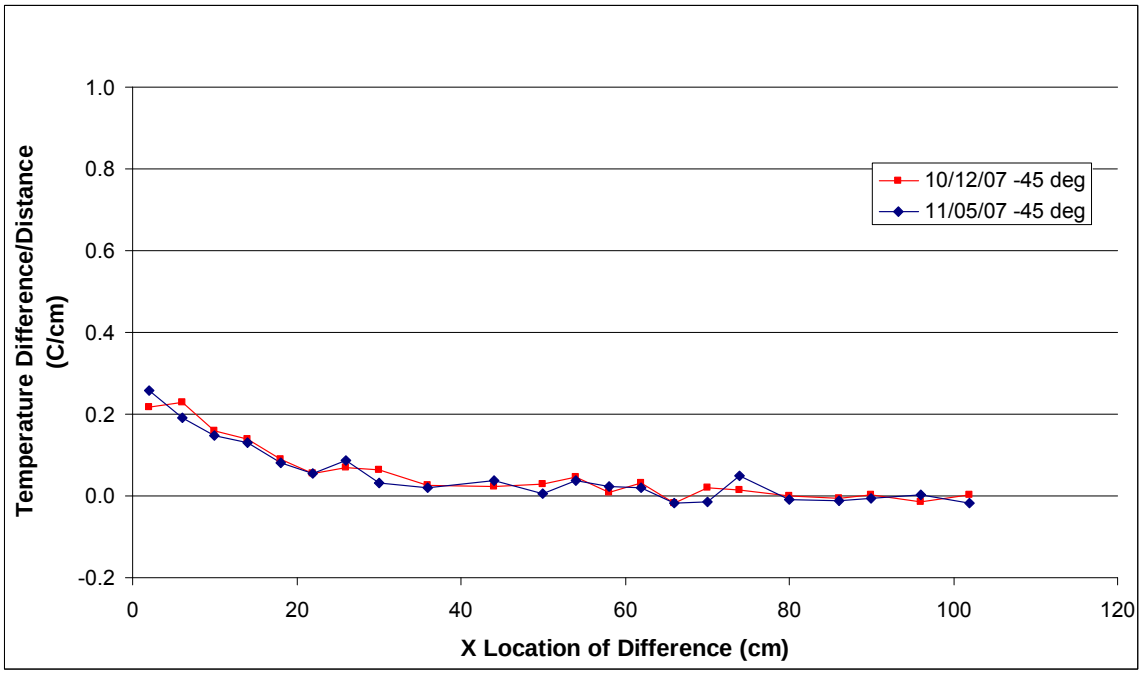

Figure 5.12 - Difference in -45° Qu Tube Temperature Divided by Distance Between Thermistors

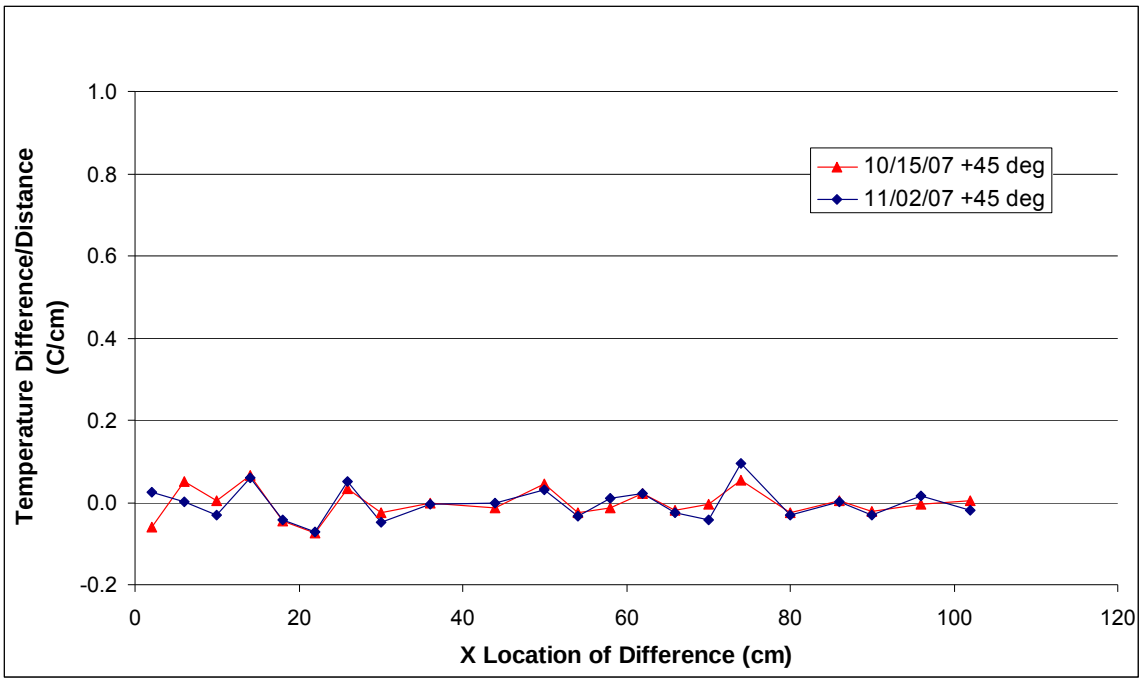

Figure 5.13 - Difference in +45° Qu Tube Temperature Divided by Distance Between Thermistors

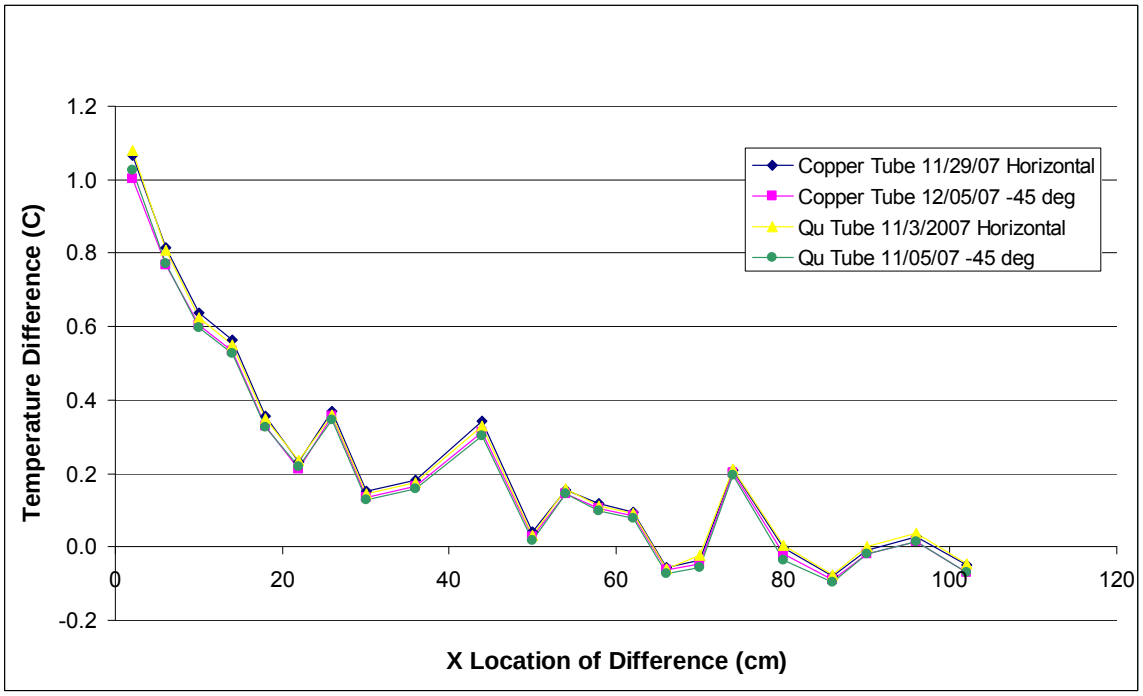

Figure 5.14 - Difference in Temperature for Qu Tube and Copper Tube

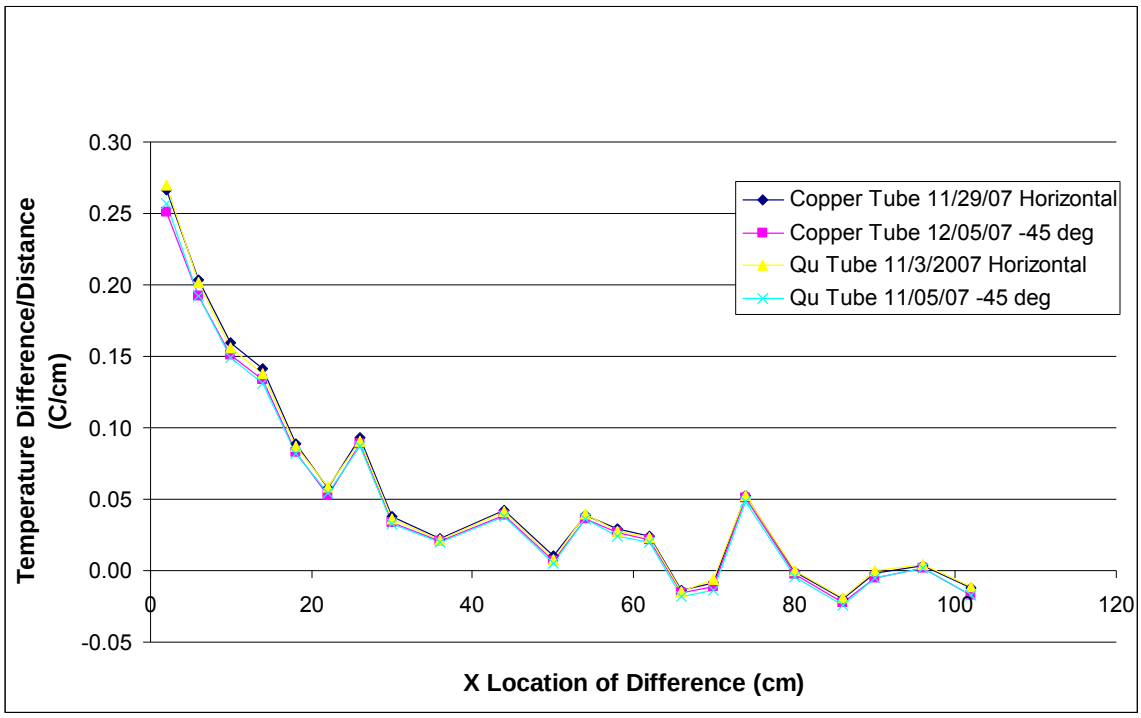

Figure 5.15 - Difference in Temperature Divided by Distance Between Thermistors for Qu Tube and Copper Tube

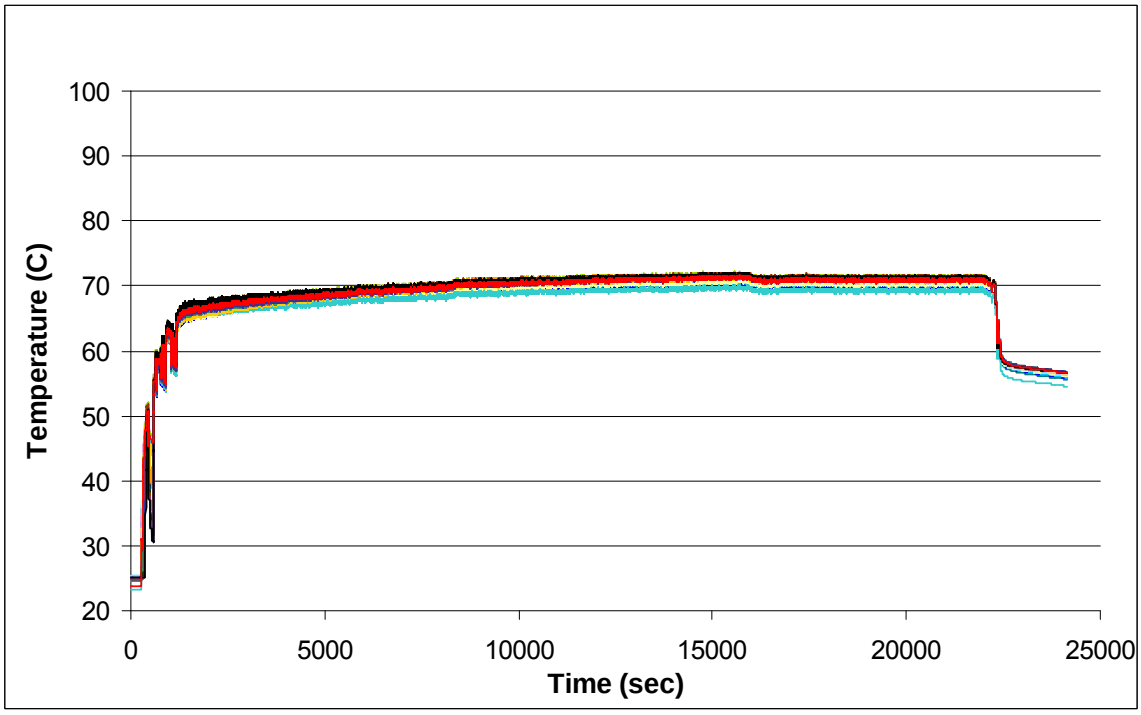

Figure 5.16 - Temperature vs. Time for the twenty-seven thermistors during a high heat rate test of the Qu Tube

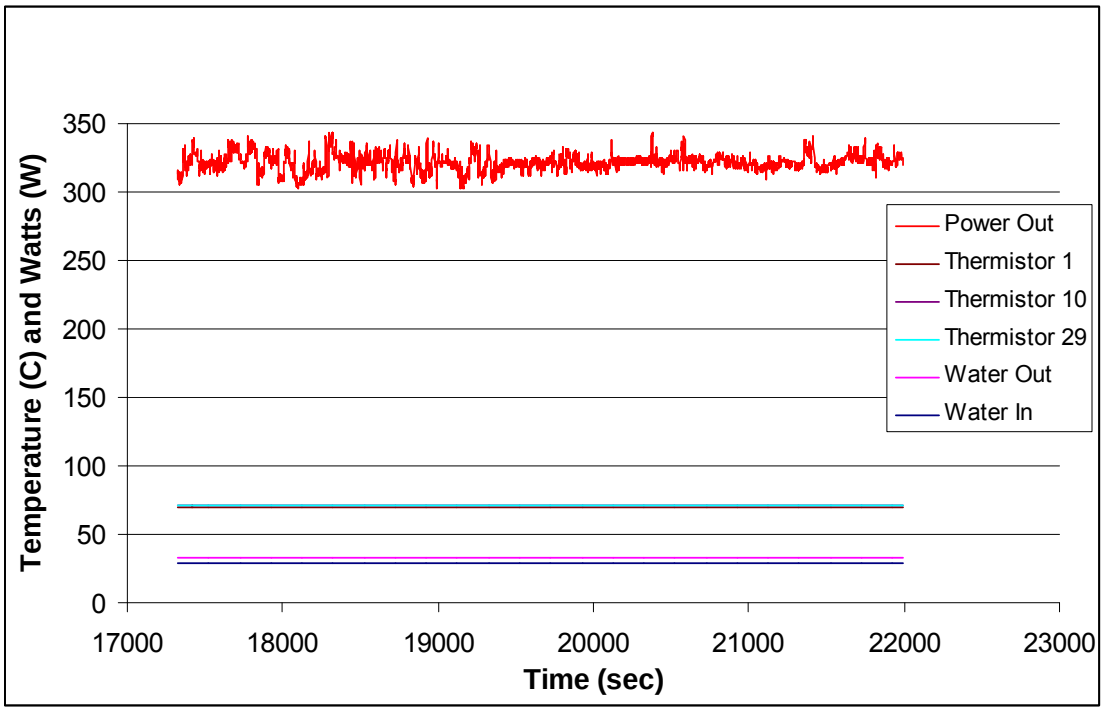

Figure 5.17 - Temperatures for Water In and Out, and Selected Thermistors, Along with Power Out Over a Steady-State Period of Time

CHAPTER 6

CONCLUSIONS AND RECOMMENDATIONS

A primary objective of this study was to develop a versatile calorimeter test apparatus for use with relatively long Qu Tubes, be able to test the tubes in the apparatus at various angles, and to accurately measure the temperatures along the Qu Tube to less than ± 1.0ºC. The UAH test apparatus, along with the thermistor calibration technique, have been shown to determine temperature differences to ± 0.14°C. Multiple tests of a Qu Tube, copper rod, and a copper tube, all 10' in length and 5/16" in diameter, have shown excellent repeatability. Using this capability it was shown that the Qu Tube has an essentially constant temperature along the length of the tube for the heat rate range of 20 to 500 W. In addition, a sinusoidal temperature gradient mentioned in previous studies (such as the SRI study referenced in Appendix A) was not found to be present. However, this could possibly be explained by the variation in the formulas for the claimed solid-state material in a Qu Tube. Another possible explanation is that the measurements in the previously mentioned study were erroneous. It has also been shown that the Qu Tubes purchased for this UAH study function as a regular copper tube when in a horizontal position, and when the heated end is elevated above the cooled end. Conversely, when the Qu Tube is at a 45º angle with the heated end below the cooled

end, very high thermal conductivities are demonstrated, as shown by the essentially constant temperature along the length. This gravity dependent effect is one of the many aspects of the Qu Tube that should be further studied. Using the capability of the UAH apparatus to be rotated while the Qu Tube is being heated, it is possible to map the performance of the Qu Tube while the angle is increased or decreased by set increments. It is possible that temperature gradients along the Qu Tube could develop between the inclinations of + 45º and horizontal if the heat transfer mechanism performance diminishes. Such gradients would allow a thermal conductivity to be determined with the existing apparatus.

High heat rate tests are essential to characterizing the performance of the Qu Tube, and in determining the Qu Tube's suitability for potential applications. The UAH testing apparatus is capable of heat rates of 5,000W, but the radial resistance the Qu Tube has to high radial heat flux hampers experiments that utilize the high heat rate capability. Having a radial thermal resistance coupled with the temperature limits of the thermal grease, insulation, and instrumentation, prevents the current apparatus from being used at heat rates above about 500W. Changes to the insulation and use of a high temperature thermal grease (or even a liquid metal) could enable higher radial heat fluxes to be achieved. However, use of Qu Tubes designed to provide a lower internal radial thermal resistance should also be considered.

A potential area for improvement in the apparatus would be the capability to "calibrate in place." Instead of calibrating thermistors in an environmental chamber, and exposing them to potentially rough handling, the thermistors and thermistor rakes would be placed on a Qu Tube and installed into a modified apparatus. The modifications

would include insulating walls that enclose the Qu Tube test assembly. Further insulation could be wrapped around the outside walls, and strip heaters could also be used to regulate the temperature inside the walls. This approach essentially turns the apparatus into an oven, and could allow the thermistors to be calibrated more precisely, while attached, or in contact with, the Qu Tube.

APPENDICES

APPENDIX A

QU ENERGY WEBSITE

- Flash Intro

QuEnergy
- About QuEnergy
- Contact Us

Technology
- QuTech™Technology
- TurboComTechnology

Products & Services
- Industrial
- Electronics
- Consumer
- Geothermal/Permafrost
- Gas Sealing Systems

References
- Press Center
- Events
- Patents
- Technology Updates

Home - **Technology**

QuTech™ Heat Transfer Technology

QuTech™ is a breakthrough in heat transfer technology. A patented mixture of inorganic compounds (Superconducting Medium) is injected into a vessel of any cross-sectional shape or material. The vessel is then vacuum-sealed to form a superconducting component. When the vessel is heated at one end, the entire vessel exhibits thermal superconductivity that causes heat transfer from the hot end of the vessel to the cold end at an extraordinary speed. The whole surface of the vessel rapidly equates to the temperature of the hot end.

Stanford Research Institute International (SRI) has verified the exceptional heat transfer performance of the superconducting component, both experimentally and by observation of installed equipment using the technology.

New Qu Energy Limited owns the patents to QuTech™ technology. Patents have been filed in the United States, Europe and other countries.

The company is continually searching for ways of utilizing thermal energy with QuTech™ and has built an advanced manufacturing plant in China for the production of QuTech™ component parts. R&D and application designs are also carried out at the plant.

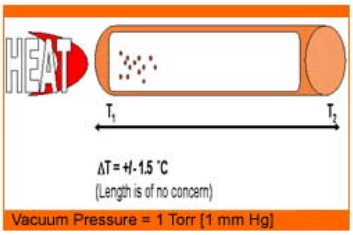

Stanford Research Institute
Validation, September 2001

QuTech™ Characteristics

- Consists of 20+ inorganic chemicals (Powder form)
- Vacuum sealed into various vessels of different sizes and material to form thermal superconducting component; QuTech™
- High thermal conductivity
- Effective Thermal Conductivity of the superconducting medium is 32,000 times that of Silver[1]
- Uniform temperature distribution
- Wide operating temperature range (-30 ~ 1100°C)

Advantages

- More efficient heat transfer
- Lower investment costs
- Reductions in costs of operation and maintenance
- Increase in overall performance and efficiency of operating equipment
- Thermal applications not possible with any other technology
- Minimum effects of orientation
- Minimum effect from gravity
- Minimum effects due to acceleration
- Non Radioactive, non toxic[2] a = 1.4 x 10-1 Bq/g, ß = 1.7 x 10-1 Bq/g (Equivalent to the radioactivity of wood)
- Maximum Heat Flux Density: 270 W/cm²
- Optimum Heat Flux Density: 158W/cm²
- Net heat loss in transmission over axial length is nearly zero
- Non-radioactive
- Non-toxic, non-poisonous
- No power required

[1] Stanford Research Institute Validation, October 2000
[2] Stanford Research Institute Validation, July 2000

Stanford Research Institute Reports

Stanford Research Institute International (SRI) has verified the exceptional heat transfer performance of the superconducting component, both experimentally and by observation of installed equipment using the technology. The following are excerpts from the SRI Reports.

1. QuTech™ Field Evaluations

"According to the facts learned and the data collected during the investigation, the investigators are convinced that the QuTech™ tubes are obviously advanced in a number of aspects and each application yielded a unique insight into the advantages of using QuTech™ tubes over conventional heat transfer technologies.

- Wide Applicable Temperature Range
- Good Compatibility with Pipe Walls
- Allows Horizontal Installations and Facilitates Automatic Cleaning
- Low Internal Thermal Resistance. Good Isothermal Characteristics
- Working Medium is not Apt to Freeze
- Overall, the QuTech™ tube is a thermal conducting element with wide applications."

2. Thermal Property Analysis of the Qu Supertube (Part 1 Studies)

"Close inspection of the axial distribution of surface temperature reveals a single period sinusoidal pattern suggestive of a standing wave. On occasions, this wave is configured in such a way that the end furthest from the heater is hottest."

"The overall performance of the Qu Supertube is inconsistent with the expected operation of a conventional heat pipe."

"It is possible, or probable that a hitherto unexplored mode or mechanism operates to transfer heat at very high rates."

3. Properties of the Qu Supertube (Phase II Studies)

"At 2.5 x 106 Wm-2, the ratio of keff to the thermal conductivity of silver was greater than 32,000, showing that the heat transfer mechanism cannot be traditional thermal conduction."

"The maximum heat flux density measured using differential calorimeters was 2.5 x 106 Wm-2. This is limited only by the inability to achieve higher input powers not by failure of the Supertube to conduct heat."

"Roughly sinusoidal temperature profiles, similar to those reported in Phase I, were seen at heat flux densities up to 2.5 x 106/m2."

4. Properties of the Qu Supertube Radiation Safety Measurement

"In summary, the total amount of radiation in the form of neutrons and gamma rays released from an operating Qu Supertube is equivalent to that produced by a heated steel pipe of similar dimension (i.e., effectively zero) and is less than that found in the ambient natural background."

5. Acute Eye Irritation Study of Super-tube Powder in Rabbits

"Super-tube Powder was classified as a nonirritant to the eye of female New Zealand White rabbits."

6. Acute Oral Limit Study of Super-tube Powder in Male and Female Mice

"Super-tube Powder at a dose level of 2000mg/kg resulted in no mortality or adverse clinical signs.....and no adverse clinical signs were observed at any time during the study."

7. Primary Dermal Irritation Study of Super-tube Powder in Male and Female Rabbits

"Super-tube Powder was classified as a nonirritant to the skin of male and female New Zealand white rabbits."

8. Acute Dermal Limit Study of Super-tube Powder in Male and Female Mice

"Super-tube Powder at a dose level of 2000mg/kg resulted in no mortality or adverse clinical signs.....and no adverse clinical signs were observed at any time during the study."

9. Evaluation of Super-tube Powder in the Murine Local Lymph Node Assay in Female CBA/Ca Mice

"Results showed that all dose levels of Super-tube powder exhibited stimulation indices below the cut-off level for a positive contact sensitizing agent."

QuEnergy International Corporation • Phone: (909) 396-8000 • Fax: (909) 396-8090 • Email: info@quenergy.net
21680 Gateway Center Drive, Suite 350 • Diamond Bar, California 91765, U.S.A.

APPENDIX B

CYLINDRICAL RADIAL CONDUCTION ANALYSIS

Heat Lost from Heater Coil Wires

Number of Coils	1			
Diameter of Coil Wire	0.1019	in	0.002588	m
k of insulation	0.1	W/m K		
Length	4	in	0.1016	m
r1 wire outer	0.05095	in	0.001294	m
r2 insulation outer	0.062	in	0.001575	m
h outer	12	W/m^2 K		
Touter (ambient)	25	C		
T1	70	C	Thickness	0.01105 in

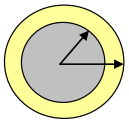

q lost **0.523449282 Watts**

Cylindrical Temperature Distribution - Mineral Wool and ULTRA Jacket 800 with Free Convection,

Number of Coils	1			
Length of Coil	8	Inch	0.2032	m
UJ 800	2	Inch Thick		
Mineral Wool	1	Inch Thick		
k of UJ800	0.0562	W/m-K		
k of Mineral wool	0.09	W/m-K		

Kreith: Pages 36-38

r_i	0.5	inches	0.0127	m
r1	0.657	Heater Coil Outer Radius, inch	1.67E-02	m
r2	1.657	Mineral Wool Outer Radius, inch	0.042088	m
r3	3.657	UJ 800 Outer Radius, inch	0.092888	m
houter	2	Free Convection Heat Transfer Coefficient		W/m^2-K
L (length of heater coils)	8	inches	0.2032	m
Touter (ambient)	25	C	Note: in this case, due to the expression for free	
T1	315	C	convection, it is necessary to use deg C.	
q lost	**12.452**	**W**	Rate of Heat Flow	
T2 - T1	-100.245			
T3 - T2	-137.258			
T3 - Touter	52.50			

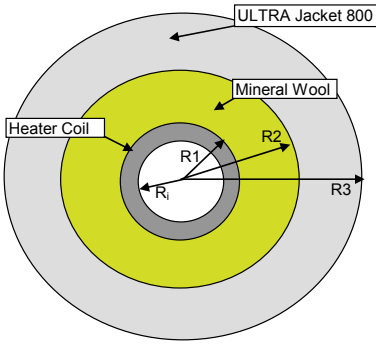

T1 =	315	
T2 =	214.75	
T3 =	77.50	171.495209

Cylindrical Temperature Distribution - Test Item with Added Insulation Inside ULTRA Jacket 800 with Free Convection,

Length	12	Inch	0.3048	m
UJ 800	2	Inch Thick		
Added Foam Insulation	1	Inch Thick		
k of UJ800	0.0562	W/m-K		
k of Foam Insulation	0.1	W/m-K		

Kreith: Pages 36-38

r1	0.15625	Test Item Outer Radius, inch	3.97E-03	m
r2	1.15625	Added Insulation Outer Radius, inch	0.029369	m
r3	3.15625	UJ 800 Outer Radius, inch	0.080169	m
houter	2	Free Convection Heat Transfer Coefficient		W/m^2-K
Touter (ambient)	25	C	Note: in this case, due to the expression for free	
T1	135	C	convection, it is necessary to use deg C.	
q lost	**4.776**	**W**	Rate of Heat Flow	
T2 - T1	-1.268			
T3 - T2	-1.131			
T3 - Touter	0.40			

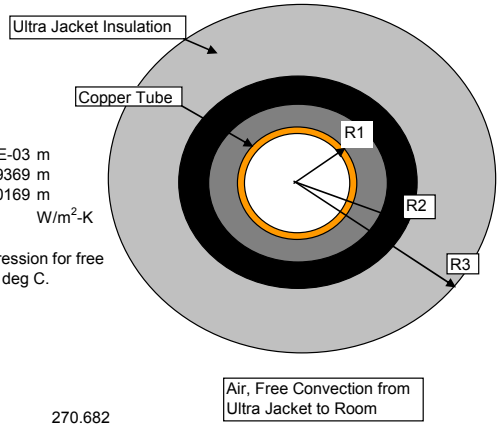

T1 =	135	
T2 =	133.73	
T3 =	132.60	270.682

Cylindrical Temperature Distribution - Delrin and Ultra Jacket 800 with Free Convection, Thermal Grease Fills Gap (0.095")

Ultra Jacket 800	2	Inch Thick			
k of UJ 800	0.0562	W/m-K			
k thermal grease	2.61	W/m-K			
k Delrin	0.23	W/m-K			
Kreith: Pages 36-38					
Diameter of Thermistor	0.095	Inch			
rgap	0.191	Inch		0.004858	m
r1	0.156	Tube Outer Radius, inch		3.97E-03	m
r2	1.848	Delrin Outer Radius, inch		0.046927	m
r3	3.848	UJ Outer Radius, inch		0.097727	m
houter	2	Free Convection Heat Transfer Coefficient			W/m^2-K
L	1.2	m			
Touter	25	C			
Tinner	30	C			
q lost	**1.3418**	**W**	Rate of Heat Flow		
Tgap - T1	0.014				
T(R)	29.99				
T measured by thermistor	29.99311				

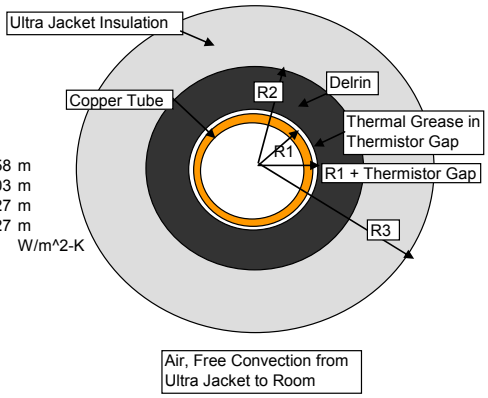

Heat Lost at Bottom of Copper Bar, Test Item, and Coil

T room	25	C	
Tcoil, etc.	315	C	
h	3.144	W/m^2-K	
Area	1.227	in^2	0.000792 m^2
q lost	**0.722**	**Watts**	

Heat Lost at Top of Copper Bar, Test Item, and Coil

T room	25	C	
Tcoil, etc.	315	C	
h	3.144	W/m^2-K	
Area	1.227	in^2	0.000792 m^2
q lost	**0.722**	**Watts**	

Heat Lost from Foam Insulated Test Item between Heater Coils and Delrin Rake Kreith: Pages 36-38

Length, Foam on Qutube	8	Inch	0.2032	m
Foam Thickness	2	Inch Thick	0.0508	m
k of foam	0.1	W/m-K		
r1 (Qu tube Outer)	0.1563	Qu Tube Outer Radius, inch	3.97E-03	m
r2	2.1563	Foam Outer Radius, inch	0.054769	m
houter	3.144	Free Convection Heat Transfer Coefficient		W/m^2-K
Touter (ambient)	25	C		
T1	33	C		

q lost **0.637293712** **Watts**

Calorimeter Cylindrical Temperature Distribution - with Foam Insulation and Free Convection

Length of Calorimeter	36	Inch	0.9144	Meters
Foam Thickness	0.5	Inch Thick	0.0127	Meters
k of foam	0.1	W/m-K		
k of CPVC	0.3	W/m-K		
CPVC Thickness	0.25	Inch Thick	0.00635	
Kreith: Pages 36-38				
$r_{i\ (CPVC)}$	2	inches	0.0127	Meter
r1 (CPVC Outer)	2.25	Calorimeter Outer Radius, inch	5.72E-02	Meter
r2	2.75	Foam Outer Radius, inch	0.06985	Meter
houter	3.144	Free Convection Heat Transfer Coefficient		W/m^2-K
Touter (ambient)	25	C		
T1	25	C		
q lost	**0**	**Watts**	**Rate of Heat Flow**	
T1 - Ti	0			
T2 - T1	0			
T2 - Touter	0.00			

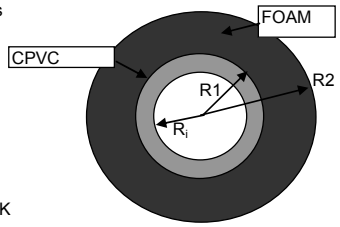

Note that for the copper tube, no heat reaches the calorimeter, and thus q = 0 at the calorimeter.

Ti =	25
T1 =	25.00
T2 =	25.00

Note: in this case, due to the expression for free convection, it is necessary to use deg C.

SUM OF LOSSES

21.174 Watts

Heat Rate from Power Supply = 21.25 Watts

APPENDIX C

PROCEDURE FOR INSTALLATION OF TEST ARTICLE

The 8" x 10' board is used as a stretcher to keep the tube supported during the transfer to the A-frame apparatus. Assembly of the test article into the apparatus starts with the 8" x 10' board laying face-up on the tables. The insulation jacket for the thermistor rakes is then placed on the board in the spot where the rakes are to be attached. With the bolts sticking up through the holes, the bottom halves of the rakes are placed on the insulation jacket, arrayed so that the thermistor wires exit the rakes going towards the top of the board, and the thermistors are then placed into the rakes. Each thermistor is inserted into its desired slot and held in place by tape. A sliver of rubber or vinyl is then place on the thermistor wire to provide stress relieving when the top half of the rake is bolted to the bottom. The AOS Heat Sink Compound 52050-1 HTC 60 thermal grease is then applied to each thermistor using a syringe. Each thermistor is then inspected to ensure it is properly aligned with the Teflon pin below it. The test article is now placed into the rakes using the pencil marks on the tube or rod as a guide to ensure consistent placement of the rakes. It is important to support the ends of the test items, especially the tubes, so as to not cause bends or kinks. The tops of the rakes are now placed onto the bottom halves, and the stress relieving cable clamp is attached to the corner bolt and

secured. The rest of the bolts are then loosely tightened. To equalize the contact resistance between the surface of the test article and the thermistors, the tube or rod is rotated slightly (a few degrees) in the direction that the thermistor wires exit, so that the thermistors are pushed and not pulled by the motion. Rotating the test item in the wrong direction can cause the thermistors to break. The bolts are then tightened and the insulation jacket folded around the rakes and fastened. U-bolts are then used to secure the insulation jacket containing the rakes to the board. Moving the board to the A-frame is a three to four person operation. The board is moved through the A-frame and then pushed up onto the U-bolt hanging down from the axle. A metal plate is slid up the bolt after the board, and held in place by two nuts.

The heater package is assembled separately. Each heater coil to be used is wrapped in foil to reduce radiation heat transfer losses, and is then placed in the mineral wool insulation. After that the insulated coils are put onto the insulation jacket, which is then wrapped around the coils and fastened. Using a flux brush, the AOS Heat Sink Compound 52027 XT thermal grease is applied to the test article. The U-bolts used to hold the heater package are then put onto the board, but not tightened down. A 5/16" OD copper rod (doesn't have to be copper) is then slid into the holes of the copper round that the heater coils are around. The rod keeps the coils aligned while the heater package is very carefully slid onto the test item. Bungee cords are used to keep the board horizontal now that the weight of the heaters has shifted the balance of the apparatus. Copper wire is tied to the end of the test item just before the first heater coil to keep the heater package from sliding when the board is tilted to different angles. Two thermocouples are placed inside the copper round, and one other is placed in between the foil and mineral wool

insulation. More mineral wool insulation is stuffed into the end of the insulation jacket, and a piece of pipe foam insulation is used to cover the hole at the end of the jacket. Three different diameters of pipe insulation are used to insulate the gap between the heater and thermistor rake insulation jackets.

At the other end of the tube, calorimeter assembly begins with the calorimeter end-cap and compression fitting nut being slid onto the tube or rod. The fin sections are then slid into position and secured using copper wire. It is important to have another person present to support the test item while this is being done, and while the calorimeter is slid on into place. U-bolts are then used to secure the calorimeter to the board. The threads of the calorimeter end-cap are then wrapped in Teflon tape and tightened into the calorimeter. Teflon tape is also used to create a compression ferrule for the compression fitting. This is done by wrapping several layers around the tube and the fitting, and then tightening the compression nut. Before adding insulation to fill the gap between the thermistor rake's insulation and the calorimeter, the water should be turned on and adjusted to different flow rates to check for leaks. The board should also be moved up and down to dislodge any air pockets.

APPENDIX D

ANALYSIS FOR INSULATED SOLID AND ANNULAR FIN TEMPERATURE GRADIENT

Boundary Condition B

Assume convection heat loss from tip is negligible, tip is treated as adiabatic.
The resulting temperature distribution for a conventional fin, with free convective heat loss is given by:

$$\frac{\theta}{\theta_b} = \frac{\cosh m(L-x)}{\cosh mL} = \frac{T-T_\infty}{T_b-T_\infty} \qquad T = T_\infty + \theta_b\left(\frac{\cosh m(L-x)}{\cosh mL}\right) \qquad \boxed{m^2 = \frac{UP}{kA_C}}$$

$$\boxed{U_{eq} = \frac{1}{\frac{r_1}{k_A}\ln\frac{r_2}{r_1} + \frac{r_1}{k_B}\ln\frac{r_3}{r_2} + \frac{r_1}{k_C}\ln\frac{r_4}{r_3} + \frac{r_1}{r_4}\frac{1}{h_4}}}$$

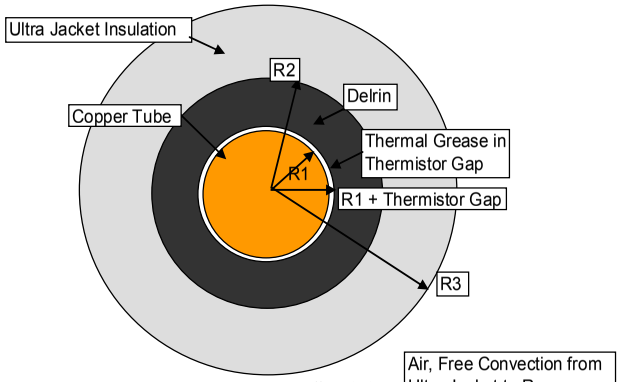

Solid Rod (Insulated)

INPUTS

	Diameter (in)	k (W/m K)	
Copper Tube	0.3125	338	
AOS Thermal Grease	0.3825	2.61	A
Delrin	2.45	0.23	B
Ultra Jacket	6.45	0.06	C

Length =	41	in
h =	1.84	W/m^2 K
T_∞ =	25	C
T_b=	48.45	C

OUTPUTS

			Radius (m)	
Copper Tube Diameter	=	0.0079375 m	0.00397	1
AOS Thermal Grease Diamter	=	0.0097155 m	0.00486	2
Delrin Diameter	=	0.06223 m	0.03112	3
Ultra Jacket Diameter	=	0.16383 m	0.08192	4

U_{eq} =	8.146266	W/m^2 K
Length =	1.0414	m
A_c=	4.95E-05	m^2
A_{eq} =	1.022392	m^2
P= A_{eq}/L =	0.024936	m
θ_b =	23.45	C
m^2 =	12.14558	1/m^2
m =	3.48505	1/m

Figure D.1 Analysis for insulated solids and annular fin temperature gradient

Solid Rod (Uninsulated)

diameter =	0.3125	in	=		0.0079375	m
Length=	41	in	=		1.0414	m
h =	12.00	$W/m^2 * K$		A_c=	4.9483E-05	m^2
k =	339	W/m * K		P= π d =	0.02493639	m
				θ_b=	23.45	C
T_∞ =	25	C		hP/kAc= m^2=	17.8384782	$1/m^2$
T_b=	48.45	C		m =	4.22356226	1/meter

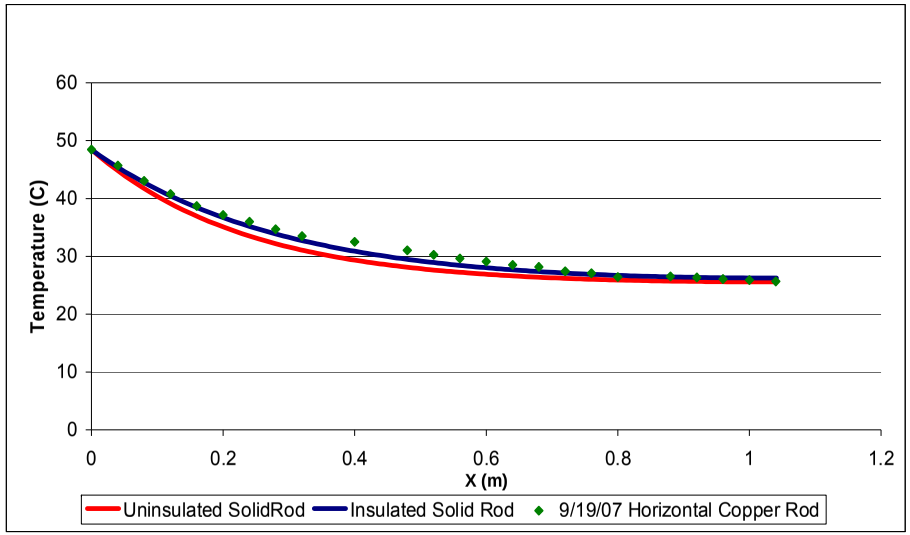

Figure D.1 Cont. Analysis for insulated solids and annular fin temperature gradient

Boundary Condition B

Assume convection heat loss from tip is negligible, tip is treated as adiabatic.
The resulting temperature distribution for a conventional fin, with free convective heat loss is given by:

$$\frac{\theta}{\theta_b} = \frac{\cosh m(L-x)}{\cosh mL} = \frac{T-T_\infty}{T_b-T_\infty} \qquad T = T_\infty + \theta_b\left(\frac{\cosh m(L-x)}{\cosh mL}\right) \qquad \boxed{m^2 = \frac{UP}{kA_C}}$$

$$\boxed{U_{eq} = \frac{1}{\frac{r_1}{k_A}\ln\frac{r_2}{r_1} + \frac{r_1}{k_B}\ln\frac{r_3}{r_2} + \frac{r_1}{k_C}\ln\frac{r_4}{r_3} + \frac{r_1}{r_4}\frac{1}{h_4}}}$$

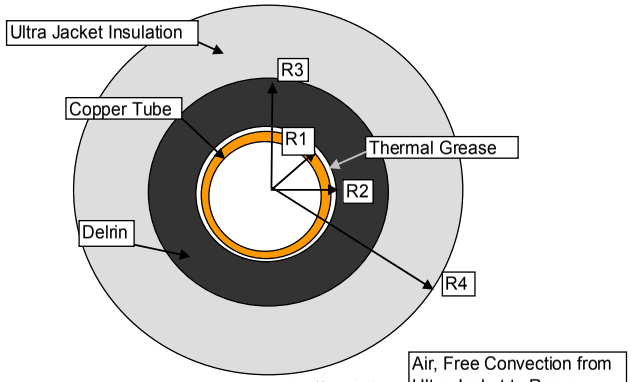

Annular (Insulated)

INPUTS

	Diameter (in)	k (W/m K)		Radius (m)	
Copper Tube	0.3125	338		0.00397	1
AOS Thermal Grease	0.3825	2.61	A	0.00486	2
Delrin	2.45	0.23	B	0.03112	3
Ultra Jacket	6.45	0.06	C	0.08192	4

Length = 41 in
h = 1.84 W/m^2 K
T_∞ = 25 C
T_b = 30 C
Wall Thickness = 0.032 in

$q = \sqrt{hPkA_c}\,\theta_b \tanh mL$ 0.38124062

OUTPUTS

Copper Tube Diameter	=	0.0079375	m	
AOS Thermal Grease Diamter	=	0.0097155	m	
Delrin Diameter	=	0.06223	m	
Ultra Jacket Diameter	=	0.16383	m	

U_{eq} = 8.146266 W/m^2 K
Length = 1.0414 m
A_c = 1.82E-05 m^2
A_{eq} = 1.022392 m^2
P= A_{eq}/L = 0.024936 m
θ_b = 5 C
m^2 = 33.03508 1/m^2
m = 5.747615 1/m
Wall Thickness = 0.000813 meter
P= πd = 0.514687 m UJ

Figure D.1 Cont. Analysis for insulated solids and annular fin temperature gradient

Annular (Uninsulated)

diameter =	0.3125	in	=		0.0079375	m
Length=	41	in	=		1.0414	m
h =	7.97	$W/m^2 * K$		A_c=	1.8193E-05	m^2
k =	339	W/m * K		P= πd =	0.02493639	m
				θ_b=	5	C
T_∞ =	25	C		hP/kAc= m^2=	32.2249375	$1/m^2$
T_b=	30	C		m =	5.67670129	1/meter
Wall Thickness=	0.032	in	=		0.0008128	meter

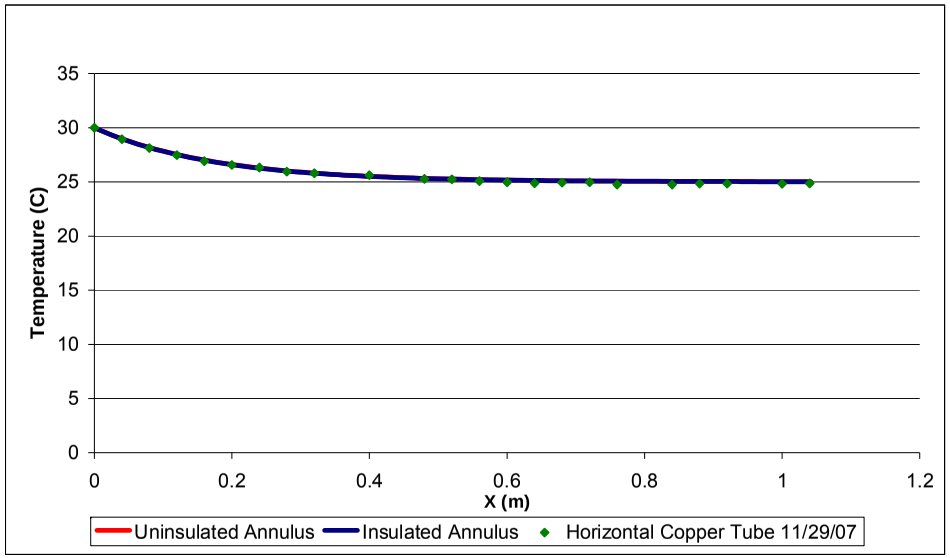

Figure D.1 Cont. Analysis for insulated solids and annular fin temperature gradient

REFERENCES

[1] Qu, Yuzhi, "Superconducting Heat Transfer Medium," Patent No. 6,132,823, dated October 17, 2000.

[2] Qu, Yuzhi, "Superconducting Heat Transfer Medium," Patent No. 6,916,430, dated July 12, 2005.

[3] Qu, Yuzhi, "Method for Producing a Heat Transfer Medium and Device," Patent No. 6,911,231, dated June 28, 2005.

[4] Qu, Yuzhi, "Medium Having a High Heat Transfer Rate," Patent No. 6,811,720, dated November 2, 2004.

[5] Enertron Inc., http://www.enertron-inc.com, accessed July 1, 2007

[6] Parker, M.L., Drolen, B.L., and Ayyaswamy, P.S., "Loop Heat Pipe for Spacecraft Thermal Control, Part 1: Vacuum Chamber Tests," *Journal of Thermophysics and Heat Transfer*, Vol. 18, No. 4, October – December 2004, pp. 417-429.

[7] Wirsch, P.J., and Thomas, S.K., "Performance Characteristics of a Stainless Steel/ Ammonia Loop Heat Pipe," *Journal of Thermophysics and Heat Transfer*, Vol. 18, No. 2, April – June 1996, pp 326-333.

[8] Hoang, T.T., and Ku, J., "Advanced Loop Heat Pipes for Spacecraft Thermal Control," AIAA Paper 2002-3094, June 2002.

[9] Coleman, H.W., and Steele, W.G., *Experimentation and Uncertainty Analysis for Engineers*, 2nd ed., Wiley-Interscience, New York, 1999.